JAERI-Tech
96-041

DEVELOPMENT OF RADIATION-HARD ULTRASONIC INSPECTION PROBES FOR ITER VACUUM VESSEL

October 1996

Koichi KOIZUMI, Masataka NAKAHIRA, Kiyoshi OKA, Kenjiro OBARA
Yutaka ITOU, Yousuke MORITA and Eisuke TADA

日本原子力研究所
Japan Atomic Energy Research Institute

本レポートは，日本原子力研究所が不定期に公刊している研究報告書です。
入手の問合わせは，日本原子力研究所研究情報部研究情報課（〒319-11　茨城県那珂郡東海村）あて，お申し越しください。なお，このほかに財団法人原子力公済会資料センター（〒319-11　茨城県那珂郡東海村日本原子力研究所内）で複写による実費頒布をおこなっております。

This report is issued irregularly.
Inquiries about availability of the reports should be addressed to Research Information Division, Department of Intellectual Resources, Japan Atomic Energy Research Institute, Tokai-mura, Naka-gun, Ibaraki-ken 319-11, Japan.

© Japan Atomic Energy Research Institute, 1996

編集兼発行　日本原子力研究所
印　　刷　㈱高野高速印刷

Development of Radiation-hard Ultrasonic Inspection Probes for ITER Vacuum Vessel

Koichi KOIZUMI, Masataka NAKAHIRA[+], Kiyoshi OKA[+], Kenjiro OBARA[+], Yutaka ITOU, Yousuke MORITA[++] and Eisuke TADA[+]

Department of ITER Project
Naka Fusion Research Establishment
Japan Atomic Energy Research Institute
Naka-machi, Naka-gun, Ibaraki-ken

(Received September 18, 1996)

The vacuum vessel of International Thermonuclear Experimental Reactor (ITER) is designed to be first safety barrier for tritium confinement. In order to assure the reliability ITER vacuum Vessel, non-destructive inspection of weld joints during in-service-inspection and after the rewelding of vessel sector for the replacement of TF coil is indispensable. Since this non-destructive inspection has to be performed by remote handling system under the intensive gamma-ray environment of more than 10^6 R/h (2.58×10^2C/kg·h) due to the radio activation of vacuum vessel, the development of radiation-hard inspection probes to satisfy high detectability, high sensitivity and sufficient long life time is essential to assure the reliability, of vacuum vessel. Based on this requirement, much efforts have been devoted for the development and testing of radiation-hard ultrasonic inspection probes which can be tolerable for more than 10^9 rad (10^7 Gy) at a dose rate of 10^6 R/h. Through a series of quality improvements and qualification tests, two types of new ultrasonic inspection probes which have sufficient and stable detectability up to 10^9 rad have been successfully developed. This report describes the structural design and irradiation test results of radiation-hard UT probes.

Keywords: Vacuum Vessel, Non-destructive Inspection, Ultrasonic Inspection Probe, Gamma Ray Irradiation, Radiation-hard UT Probe

+ Department of Fusion Engineering Research
++ Department of Material Development, Takasaki Radiation Chemistry Research Establishment

ＩＴＥＲ真空容器用耐放射線性超音波探傷素子の開発

日本原子力研究所那珂研究所ＩＴＥＲ開発室
小泉　興一・中平　昌隆[+]・岡　　潔[+]・小原健治郎[+]
伊藤　　裕・森田　洋右[++]・多田　栄介[-]

（１９９６年９月１８日受理）

国際熱核融合実験炉（ＩＴＥＲ）のプラズマ真空容器は、安全性の観点からトリチウム閉じ込めの第一隔壁としての機能を要求される。このため供用期間中の定期検査（ISI）時及びトロイダル磁場コイル交換時の再溶接完了時に現地溶接部の非破壊検査を行い、隔壁の健全性を担保することが要求される。これらの非破壊検査は、真空容器の放射化に伴い、10^6R/h(2.58×10^2C/kg·h)以上の高放射線環境下で遠隔保守にて行われる。このため、真空容器の健全性を担保するためには、高放射線環境下で高い検出精度、安定性、耐久性を有する耐放射線性非破壊検査素子の開発が不可欠である。この要請に基づき、日本原子力研究所では、10^6R/hの線量率条件下で10^9rad（10^7Gy）以上の耐久性を有する耐放射線性超音波探傷素子の開発を目標に、耐放射線性素子の設計・試作作業と並行して高崎研究所照射施設を用いた性能評価試験を続けている。これらの開発作業の結果、構造と材料構成を改良した２種類の超音波探傷素子が上記環境下で10^9radまで安定した検出感度特性を満足することを確認した。本報告は、新規に開発した２種類の耐放射線性超音波探傷素子の構造設計とガンマ線環境下での性能評価試験結果を報告するものである。

那珂研究所：〒311-01　茨城県那珂郡那珂町向山801-1
＋　核融合工学部
＋＋　高崎研究所材料開発部

Contents

1. Introduction 1
2. Qualification of Conventional Ultrasonic Probes 1
2.1 Test Conditions 1
2.2 Irradiation Test Results of Perpendicular Inspection Probes 3
2.3 Irradiation Test Results of Angular Inspection Probes 4
3. Development Radiation-hard Inspection Probes 6
3.1 Design of Radiation-hard Probes 6
3.2 Test Results in Normal Operating Condition 8
3.3 Test Results Obtained by Irradiation Test 9
4. Conclusion 13
Acknowledgements 13
Reference 13

目　　次

1. はじめに 1
2. 従来型超音波探傷素子の性能評価試験 1
2.1 試験条件 1
2.2 垂直入射型探傷素子の照射試験結果 3
2.3 斜角入射型探傷素子の照射試験結果 4
3. 耐放射線性探傷素子の開発 6
3.1 耐放射線性探傷素子の設計 6
3.2 通常環境下での性能評価試験結果 8
3.3 ガンマ線環境下での性能試験結果 9
4. 結　論 13
謝　辞 13
参考文献 13

1. Introduction

In the design of the International Thermonuclear Experimental Reactor (ITER), the vacuum vessel is designed to be a double-walled structure composed of inner skin, outer skin and poloidal ribs. A torus structure of vacuum vessel is segmented into 20 toroidal sectors spliced at the port center between the adjacent Toroidal Field (TF) magnets and they are assembled field welding at on-site. Since the vacuum vessel is expected to be a first safety barrier for tritium confinement, non-destructive inspection of weld joints for in-service-inspection (ISI) is essential technology to assure the structural integrity of vacuum vessel. In addition to ISI, the non-destructive inspection is also required after the cutting and rewelding of the field joint for re-assembly of a vessel sector when a TF magnet is replaced. These non-destructive inspection of weld joints has to be performed by remote handling system under gamma-ray irradiation condition of more than 10^6 R/h due to the radio activation of vacuum vessel by D-T operation. Therefore, the development of non-destructive inspection methods to satisfy high flaw detectability, high sensitivity and sufficient length of lifetime is indispensable for maintaining the reliability of ITER vacuum vessel. For this reason, extensive irradiation tests and quality improvements [1] including optimization of material composition have been performed in Japan Atomic Energy Research Institute (JAERI) to develop a radiation-hard inspection probe for non-destructive inspection. The major efforts of these activities were focused on the development of ultrasonic test (UT) inspection probes which can be tolerable for more than 10^9 rad at a dose rate of 10^6 R/h. In parallel with the design and trial fabrication of radiation-hard inspection probes, their performance under gamma ray environment were evaluated by using ^{60}Co irradiation test facility in Takasaki Research Establishment in JAERI. This report describes the major results obtained through the development of radiation-hard ultrasonic inspection probes.

2. Qualification of conventional ultrasonic probes

2.1 Test conditions

The non-destructive inspection with ultrasonic probe is a conventional inspection method to detect internal flaws of weld joint and base metal. The major feature of this method is to detect the size and location of internal flaw by detecting the height and time delay of echo signal reflected by the defect. In the case when ultrasonic inspection method is applied to the weld joint of stainless steel, the detectable flaw size is unfortunately more than 20 % of total wall thickness. By optimizing the peak wave frequency and band width of frequency, one inspection

1. Introduction

In the design of the International Thermonuclear Experimental Reactor (ITER), the vacuum vessel is designed to be a double-walled structure composed of inner skin, outer skin and poloidal ribs. A torus structure of vacuum vessel is segmented into 20 toroidal sectors spliced at the port center between the adjacent Toroidal Field (TF) magnets and they are assembled field welding at on-site. Since the vacuum vessel is expected to be a first safety barrier for tritium confinement, non-destructive inspection of weld joints for in-service-inspection (ISI) is essential technology to assure the structural integrity of vacuum vessel. In addition to ISI, the non-destructive inspection is also required after the cutting and rewelding of the field joint for re-assembly of a vessel sector when a TF magnet is replaced. These non-destructive inspection of weld joints has to be performed by remote handling system under gamma-ray irradiation condition of more than 10^6 R/h due to the radio activation of vacuum vessel by D-T operation. Therefore, the development of non-destructive inspection methods to satisfy high flaw detectability, high sensitivity and sufficient length of lifetime is indispensable for maintaining the reliability of ITER vacuum vessel. For this reason, extensive irradiation tests and quality improvements [1] including optimization of material composition have been performed in Japan Atomic Energy Research Institute (JAERI) to develop a radiation-hard inspection probe for non-destructive inspection. The major efforts of these activities were focused on the development of ultrasonic test (UT) inspection probes which can be tolerable for more than 10^9 rad at a dose rate of 10^6 R/h. In parallel with the design and trial fabrication of radiation-hard inspection probes, their performance under gamma ray environment were evaluated by using ^{60}Co irradiation test facility in Takasaki Research Establishment in JAERI. This report describes the major results obtained through the development of radiation-hard ultrasonic inspection probes.

2. Qualification of conventional ultrasonic probes

2.1 Test conditions

The non-destructive inspection with ultrasonic probe is a conventional inspection method to detect internal flaws of weld joint and base metal. The major feature of this method is to detect the size and location of internal flaw by detecting the height and time delay of echo signal reflected by the defect. In the case when ultrasonic inspection method is applied to the weld joint of stainless steel, the detectable flaw size is unfortunately more than 20 % of total wall thickness. By optimizing the peak wave frequency and band width of frequency, one inspection

probe can cover the inspection of the defects exist in different depth. Based on these advantageous features, UT inspection method is selected as the reference method to qualify the field joints of ITER vacuum vessel. This method is being employed for the ISI of commercial fission reactor. However, the current application to irradiation condition is limited to the dose level of less than 10^3 R/h. The operating conditions of UT probes in the ITER are summarized in Table 2.1. As shown in the table, dose rate in the ITER is three order higher than that of commercial fission reactor and there was no existing database on the radiation hardness of conventional UT proves under the dose rate of more than 10^3 R/h. For this reason, gamma-ray irradiation test has been performed to qualify the applicability of conventional UT probes to the ITER operating conditions.

Gamma-ray irradiation tests of conventional inspection probes were performed by using ^{60}Co irradiation test facility (Hot cell No. 2) in Takasaki Research Establishment in JAERI. Irradiation conditions of the UT probes in the ^{60}Co irradiation test facility are summarized in Table 2.2.

Typical two types of UT probes, perpendicular beam injection type and angular beam injection type, were employed for the testing. The configuration of perpendicular and angular inspection probe installed in the test box are shown in Fig. 2.1 and Fig. 2.2, respectively. During the gamma ray irradiation test of angular inspection probes, ultrasonic wave is injected to test sample with a angle of 45 degree. In both types of inspection probes, the same oscillator made of $PbNb_2O_6$, which has a peak frequency of 3.0 MHz, was employed for the wave source. As shown in the figures, both types of probes were set in the test box with a distance of 20 mm from the bottom surface of test box to detect the echo reflected from the bottom of test box. For evaluating the effects of couplant material on the sensitivity, two boxes were prepared for each type of probe and each of them were filled with water and glycerol, respectively. For the testing of angular inspection probes, two types of wedge material, conventional acrylic and radiation-hard PEI (polyether-imide), were employed to evaluate the effects of wedge material on the sensitivity and stability. Two UT probes were installed in each test box so as to obtain sufficient database on irradiation effects. The combination of couplant and wedge materials in each test box are summarized in Table 2.3. The data accumulation system prepared for the irradiation test is schematically shown in Fig. 2.3. The height of beam echo, beam detection time, and frequency characteristics such as the change of peak frequency and band width, were monitored and accumulated into a personal computer. Picture of test boxes installed in the ^{60}Co irradiation test facility and the view of data acquisition system are shown in Fig. 2.4.

2.2 Irradiation test results of perpendicular inspection probes

The irradiation effects of the probes on the height of beam echo, beam detection time, and frequency characteristics such as the change of peak frequency and band width, were analyzed after irradiation test. The changes of echo height represent the change of probe sensitivity. The change of echo height measured in the irradiation test are shown in Fig. 2.5. The echo height measured after the irradiation are normalized by the value of initial echo measured before the irradiation. In the case when the probes are installed in the box filled with water, the echo height slightly increased just after starting the irradiation and then decreased rapidly. The total doses corresponding to the 50 % of initial echo is 10^8 rad. The increase of sensitivity at the starting point were considered to be caused by temperature rise due to irradiation. The echo height after the irradiation of 10^9 rad , the echo height reaches to less than 10 % of initial value. In the case when the probes are installed in the box filled with glycerol, their characteristics were very similar to those of the probes installed with water. Judging from this comparison, the difference due to contact medium is small and negligible. The changes of beam detection time is shown in Fig. 2.6. As shown in the figure, the irradiation effect of the probe on the beam detection time, was very small in both contact medium. The peak frequency of UT probes was constant up to 10^8 rad. However, the values were not stable in the region of more than 10^8 rad. Also, in the dose region of more than 10^8 rad, the band width of ultrasonic wave decreased. This result reveals the wave characteristics of ultrasonic probes is not reliable over 10^8 rad. Based on these results, The lifetime of the conventional perpendicular inspection probes is estimated to be about 10^8 rad.

In order to investigate the technical reason which causes the degradation of echo height and changes in the wave characteristics, the test box and inspection probe were disassembled after the irradiation test for visual inspection. Appearances of the inside of test boxes and probes after gamma-ray irradiation up to 1.25×10^9 rad are shown in Fig. 2.7. A picture of left side corresponds to the appearance of test box filled with glycerol and the right side shows the view of test box filled with water. In case of the test box filled with water, picture shows some suspended solids in water. But, there were no change in the volume of water. On the contrary, in case of the glycerol immersion, decomposition and evaporation of glycerol due to irradiation were observed. Since no damage of probe was found by visual inspection, the casing of probe was cut and the inside of probe was checked carefully. The pictures inside of the probe is shown in Fig. 2.8. As shown in the figure, the damage of bonded surface

between the oscillator ($PbNb_2O_6$) and protector was found due to the radiation damage of adhesion made of epoxy resin. Also the cracks were found between the damper (powdered W in epoxy) epoxy filler. Based on these inspections, it was concluded that the degradation of probes is generated by the radiation damage of epoxy used for adhesive and filler material.

2.3 Irradiation test results of angular inspection probes

Fig. 2.9 shows the changes of echo intensity of angular probes as a function of total doses. Comparing with the data obtained in the test of perpendicular probes, it is shown that the degradation of echo intensity begins immediately after starting the irradiation. In the case when acrylic is employed for wedge material (Ch-6 and Ch-8), this degradation became faster than those of the probe with PEI wedge and the echo intensity decreased to 50 % of initial echo at 10^7 rad. Also, the echo heights became almost zero at 10^9 rad. On the contrary, in the case of radiation-hard PEI (polyether imide) type, the degradation phenomena were similar to those of perpendicular probes, and total dose corresponds to 50 % of the initial echo was 10 times larger than those of the probe with acrylic wedge. The recovery of echo intensity observed in Ch-5 at 10^9 rad is considered to be generated by the recovery of couplant at contact surface. Regarding the effects of couplant, it is shown that the degradation of sensitivity measured with glycerol was little smaller than the values measured with water. The change of beam detection time are presented in Fig. 2.10 as a function of the total doses. As shown in the figure, the detection time of all angular probes became longer due to gamma-ray irradiation. This means the velocity of ultrasonic wave changes and becomes slow due to the gamma-ray irradiation. However, in the case when acrylic is employed for wedge material , ultrasonic beam was not detected at 10^9 rad. The peak frequency of angular inspection probes were constant up to 10^7 R however, it became unstable in the region of more than 10^7 rad. The characteristics of frequency band width under irradiation showed similar characteristics of perpendicular probes. Based on these results, it was expected that the reliable life time of angular probe is, 10^7 rad and 10^8 rad for the probe with acrylic wedge type and PEI wedge type, respectively.

In order to investigate the technical reason which causes the degradation of sensitivity, the condition of angular type probes were also checked by visual inspection. View of the angular inspection probes after gamma ray irradiation test up to 10^9 rad is shown in Fig. 2.11. As shown in the figure, the irradiation damage of angular type probes is more serious than those of perpendicular type. In case acrylic

wedge type, wedge material was melted away due to radiation damage and oscillator is exposed in the medium. Cross sectional view of angular probe, which has acrylic wedge, is shown in Fig. 2.12. As seen in the figure, almost all acrylic material was melt down and no wedge material exist in the interface at 10^9 rad. Also, many porous structure is observed in the epoxy filler due to swelling under gamma ray irradiation. The condition of angular probes with PEI for wedge is shown in Fig. 2.13. Although small deformation of casing is observed due to the swelling of epoxy filler, no serious damage is observed in the wedge material. According to these inspections, it was concluded that the employment of radiation-hard material and reduction of epoxy are essential to develop radiation-hard ultrasonic probe applicable to ITER operating conditions.

Table 2.1 The conditions of the non-destructive inspection in ITER

Dose rate in irradiation	~10^6 R/h
Total dose	~10^9 rad
Atmosphere	air or inert gas (nitrogen)
Pressure	1 bar
Temperature	50 ~150 °C

Table 2.2 Irradiation conditions of the UT probes

	Condition
1. Gamma ray irradiation dose rate: a) Perpendicular inspection probe b) Angular injection probe	 1.04 x 10^6 R/h 1.06 x 10^6 R/h
2. Irradiation duration	~ 1200 hours
3. Total exposure	1.25 ~ 1.27 x 10^9 R
4. Temperature range during irradiation test:	30°C ~ 40°C

Table 2.3 Combination of couplant and wedge materials

Unit No. of test box	Type of probe	Couplant	Wedge material	Total number of probes
1	perpendicular	Water	None	2
2	perpendicular	Glycerol	None	2
3	angular	Water	PEI	1
			Acrylic	1
4	angular	Glycerol	PEI	1
			Acrylic	1

3. Development radiation-hard inspection probes

3.1 Design of radiation-hard probes

Based on the results obtained by the irradiation test of conventional ultrasonic inspection probes, the development of new radiation-hard probe has been initiated. The target of the development are summarized in Table 3.1. Since the angular type probe is more convenient for the inspection of the field joint between vacuum vessel sectors, the design and development work were focused on the development of angular type inspection probe.

Table 3.1 Target of the development

Design item	Target value
Detectability of flaw size (with water couplant or dry couplant)	more than 10% of total thickness > 3 mm for SS316 > 4 mm for Inconel 625
Radiation hardness	more than 10^9 rad at 106 R/h
Operation temperature	more than 50°C
Peak frequency	~ 2 MHz
Band width of frequency	2 ~ 3 MHz
Refraction angle	~45°
Dimensions - Probe height - Probe width	 less than 70 mm less than 50 mm

Two configurations of angular inspection probe, Type-A and Type-B, designed for ITER application, are shown in Fig. 3.1 and Fig. 3.2, respectively. The major features of the structural design of Type-A and Type-B are listed below;

Type-A

1) No epoxy filler in the structure for holding oscillator and damper
2) No adhesion between wave source and damper
3) Wavy-shaped damper to reduce noise signal
4) Minimum use of epoxy resin

Type-B

1) High mechanical integrity with modular structure
2) Epoxy filler for high temperature use
3) Wavy-shaped damper to reduce noise signal
4) Minimum use of epoxy resin

In the design of Type-A, a mechanical support concept of oscillator and damper without filler was employed to reduce the amount of epoxy. As shown in Fig. 3.1, both components and the contact surface between damper and oscillator are support by holding screw. Since the basic configuration of Type-A has no filler, steel casing was designed to protect key components of the probe. Also, the cable supporting structure and support base were designed to assure the reliability of electrical connection. In addition to this improvement, radiation-hard material such as PEI (polyether imide) and PI (poly imide) were employed for wedge material. The mechanical characteristics of PEI and PI employed for the fabrication are summarized in Table 3.2. Both materials have stable characteristics under gamma ray irradiation environment and the degradation of tensile strength of PEI is about 6 % up to the total dose of 5×10^8 rad at 10^6 R/h. The mechanical characteristics of PI are stable up to 1×10^9 rad. In the design of Type-B, the modular structure which is composed of perpendicular inspection probe and wedge was designed. Both components are mechanically connected by steel screw. In this structure, the ultrasonic wave is transmitted to wedge through the radiation-hard couplant. Radiation-hard materials are also employed for wedge material. The use of epoxy for damper and filler is also minimized.

Table 3.2 Mechanical characteristics of PEI and PI employed for the fabrication

	PEI (ULTEM)	PI (CEPLA)
Absorption of water	0.25 % (23°C, 24 hr)	0.46 % (20°C, 48 hr)
Tensile strength	123 MPa	116 MPa
Elongation	23%	5 %
Bending strength	157 MPa	161 MPa
Bending elasticity	3.0 GPa	4.17 GPa
Compressive strength	118 MPa	26.5 MPa (1% strain)
Compressive elasticity	3.3 GPa	2.6 GPa
Thermal contraction ratio	5.6×10^{-5} (-18°C~ 150°C)	3.62 (20~100°C) 6.35 (100~200°C)

3.2 Test results in normal operating condition

The performance of newly developed radiation-hard probes were evaluated under normal operating condition before irradiation. Test sample used for the evaluation of sensitivity of the probes is shown in Fig. 3.3. For this test, two different materials, Inconel 625 and SS316, are selected because of the candidate structural materials for ITER vacuum vessel. As shown in Fig. 3.3, each test sample has two types of artificial defects, side drill hole (SDH) and slit machine by electrical discharge machining (EDM) . The sizes of these defects (1.5~9.0 mm) corresponds to, 5%, 10%, 15%, 20% and 30% flaw to the total thickness. In order to evaluate the effects of wedge materials on the sensitivity and stability, the additional probes of Type-A and Type-B, which employ acrylic material for wedge, have been fabricated and tested with the PEI type and PI type. The major characteristics of the fabricated inspection probes measured by using the standard test sample (TYPE: STB-A1) of the Japanese Industrial Standard (JIS) Z2345 are summarized in Table 3.3.

Table 3.3 Major characteristics of the fabricated inspection probes

Probe Type	Probe No.	Wedge Material	Refraction Angle	Peak Frequency	Band width of inspection frequency
Type-A	No. 1	PEI	46.0°	1.96 MHz	2.03 MHz
	No. 2	PEI	46.5°	1.80 MHz	2.11 MHz
	No. 3	PEI	45.5°	1.96 MHz	2.35 MHz
	No. 4	PEI	46.0°	2.03 MHz	2.19 MHz
	No. 5	PI	45.0°	1.96 MHz	2.19 MHz
	No. 6	PI	44.9°	2.11 MHz	2.11 MHz
	No. 7	PI	44.8°	2.19 MHz	2.90 MHz
	No. 8	PI	44.2°	2.03 MHz	2.26 MHz
	No. 9	Acrylic	45.5°	1.88 MHz	2.11 MHz
	No. 10	Acrylic	45.5°	1.96 MHz	2.27 MHz
Type-B	No. 1	PEI	45.0°	2.19 MHz	2.90 MHz
	No. 2	PEI	45.8°	3.05 MHz	3.80 MHz
	No. 3	PI	45.5°	2.19 MHz	2.74 MHz
	No. 4	PI	45.0°	2.50 MHz	3.29 MHz
	No. 5	Acrylic	45.0°	1.96 MHz	2.42 MHz
	No. 6	Acrylic	45.0°	2.03 MHz	2.97 MHz

The sensitivity of the angular probe Type-A on the various size of flaw is measured at room temperature. Test results are shown in the figures from Fig. 3.4 to Fig. 3.8. In these figures, the sensitivity represented by the echo height are normalized by the height of the echo measured with standard test sample (STB-A1). From these figures, the sensitivity for the slit-type defects (SDH) is much higher than the sensitivity to the hole-type defects (EDM). This characteristic does not depend on the wedge material. Also, the difference due to wedge material is not observed. It is shown that Type-A has the sensitivity of more than 20 % for 10% defect in SS316 plate. Test results obtained by the angular probe Type-B are also presented in figures from Fig. 3.9 to Fig. 3.11. As shown in the figures, the major characteristics of Type-B are similar to those of Type-A and no difference on the sensitivity characteristics was found in the test. It is also shown that Type-B also has sufficient sensitivity to 10 % flaw in 30 mm-thick SS316 plate. Based on these results, it was concluded that the newly developed ultrasonic probes, Type-A and Type-B, have sufficient sensitivity under non-irradiation environment.

3.3 Test results obtained by irradiation test

(1) Test conditions

After the evaluation test in normal operating condition, the gamma-ray irradiation test of newly developed probe, Type-A and Type-B, were conducted in the ^{60}Co irradiation test facility in Takasaki Research Establishment in JAERI. Irradiation conditions of the UT probes at the ^{60}Co irradiation test facility are summarized in Table 3.4. The same data acquisition system mentioned in Section 2.1 has been employed for the measurement. In order to evaluate the effects of wedge materials, the additional probes of Type-A and Type-B, which employ acrylic material for wedge, have been fabricated and tested with the PEI and PI types. The view of the inspection probes installed in the hot cell is shown in Fig. 3.12. Since the continuous monitoring of the sensitivity to various flaw sizes was difficult due to limit of available space in the hot cell, the performance tests were conducted by using the interval between the operation of hot cell.

(2) Test results of Type-A

a) Irradiation effects on sensitivity

Changes of the sensitivity of a inspection probe Type-A under gamma-ray irradiation are measured for several size of defect machined in SS316 test sample. The test results are shown in figures from Fig. 3.13 to Fig. 3.17 as a function of total

Table 3.4 Irradiation conditions of the UT probes

	Condition
1. Gamma ray irradiation dose rate	1.05×10^6 R/h
2. Total doses	~ 1.0×10^9 R
3. Temperature during irradiation test	30°C ~ 40°C

dose. The sensitivity to the 5 %, 10 % and 20 % defects, are normalized by the initial sensitivity to the 30% defect. In the wedge material of PEI and PI, the degradation of the sensitivity is not observed up to 1×10^9 rad. In the dose range of more than 10^8 rad, however, the increase of the sensitivity is also observed with the increase of total dose. This characteristic does not depend on the defect type and wedge materials. The increase of the sensitivity means that the degradation of beam energy due to wedge is decreased by gamma ray irradiation. This improvement of the sensitivity is considered to be generated by the irradiation hardening of wedge material. In the wedge material of acrylic, the signals are no longer obtain in the dose range of more than 1.5×10^8 rad. This dose limit of the probe with acrylic wedge is almost equal to the values obtained by the irradiation test of conventional inspection probe. The picture of the inspection probe Type-A which were taken before and after the irradiation test up to 1×10^9 rad are shown in Fig. 3.18. As shown in the figure, no damage was found in the PEI and PI type however, the deformation, discoloration and melting of the wedge are observed in the acrylic type after the completion of irradiation test.

b) Irradiation effects on beam path length

The changes of beam path length measured in the irradiation test of Type-A probes which have PEI wedge PI wedge are shown in Fig. 3.19 and Fig. 3. 20 as a function of total dose. The beam path length corresponds to the speed of ultrasonic wave in the materials. In normal operating environment, beam path length depends on the flaw size of SDH since the difference of defect diameter makes the change of path length. Also the path length is constant for the slit-type defects since the distance between probe and artificial defect is constant. As shown in Fig. 3.19 and Fig. 3.20, these basic characteristics of beam path length to two types of defects are also maintained in the irradiation test of Type-A. The values of beam path length measured for each defect size were almost constant in the irradiation test and serious irradiation

effects on beam path length was not observed. Also, the comparison of the data obtained by PEI type and PI type showed that the beam path length does not depend on the wedge material.

c) Irradiation effects on refraction angle

The refraction angle is determined by the speed of ultrasonic wave in wedge material and test sample. In the case when the same test sample is employed for measurement, the change of refraction angle represents the irradiation effects on wedge material. From this point of view, the change of the beam refraction angle was measured by standard test sample. In wedge material of acrylic, the refraction angle of decreased with the increase of total dose, while the those of PEI and PI, the values were constant up to 1 x 10^9 rad. From these results, it was verified that the application of PEI and PI for wedge material is effective to improve the radiation hardness of ultrasonic probe.

d) Irradiation effects on peak frequency and band width

The changes of peak frequency and band width due to the irradiation are mainly caused by the change of bonding conditions between wave source and damper, between wave source and wedge material. Also, they depend on the condition of initial assembly during fabrication. For these reasons, the change of peak frequency and band width due to irradiation were analyzed with FFT analyzer. In the PEI wedge, three probes showed almost constant peak frequency and band width up to 1 x 10^9 rad however, while one of four probe showed the decrease and recovery during the irradiation test. In the case of PI type, one probe showed unstable characteristics in the irradiation test but the other three showed stable characteristics up to 1 x 10^9 rad. The results showed that the characteristic change due to the irradiation strongly depends on the difference of initial conditions, and further improvement of the bonding conditions between the wave source and damper and/or between wave source and wedge material, are required to obtain reliable performance under gamma-ray irradiation.

(3) Test results of Type-B

a) Irradiation effects on sensitivity

Changes of the sensitivity of an inspection probe Type-B due to gamma-ray irradiation are measured for the artificial defects in SS316 test sample. Test results are shown in the figures from Fig. 3.21 to Fig. 3.23 as a function of total dose. In the

wedge material of PEI and PI, the degradation of sensitivity is not observed up to 10^9 rad. In the dose range of more than 10^8 rad, the increase of the sensitivity observed in testing of Type-A was also confirmed in Type-B. This characteristic did not depend on the defect type and wedge materials. In the wedge material of acrylic, the sensitivity decreased with the increase of total dose and no sensitivity was obtain in the dose range of more than 1.5×10^8 rad. No significant differences between sensitivity of Type-A and B. The View of angular inspection probe Type-B after the irradiation test up to 1×10^9 rad is presented in Fig. 3. 24. As shown in the figure, no damage was found in the PEI and PI type however, the deformation and discoloration of wedge is observed in the acrylic type after the completion of irradiation test.

b) Irradiation effects on beam path length

The changes of beam path length measured in the irradiation test of Type-B probes which have PEI wedge PI wedge are shown in Fig. 3.25 and Fig. 3. 26 as a function of total dose. From the figures, basic characteristics of beam path length to two types of defect are similar to those of Type-A. The values of beam path length measured for different defect sizes were almost constant in the irradiation test and serious irradiation effects on beam path length was not observed. Also, it was shown the beam path length does not depend on the wedge material.

c) Irradiation effects on refraction angle

The change of the beam refraction angle was measured with standard test sample. The refraction angle of acrylic type decreased with the increase of total dose however, the refraction angle of PEI type and PI type were constant up to 1×10^9 rad. These characteristics are similar to those of Type-A. The comparison of the characteristics also showed that there are no significant differences between Type-A and B regarding the irradiation effect on refraction angle.

d) Irradiation effects on peak frequency and band width

The changes of peak frequency and band width due to the irradiation were analyzed with FFT analyzer. Two probes with PEI and PI were tested and one of each type showed the constant peak frequency up to 1×10^9 rad however, the other one showed the decrease and recovery of peak frequency during the irradiation test. The stability of Type-B is lower than those of Type-A.

4. Conclusion

Based on the results obtained by the irradiation test of conventional ultrasonic inspection probes at 10^6 R/h, two types of radiation-hard probe, Type-A and Type-B, have been successfully developed. The characteristics of these radiation-hard probes were measured in normal and gamma-ray irradiation conditions. Through the series of testing on conventional and newly developed radiation-hard ultrasonic probes, the following conclusion were obtained;

(1) In the gamma ray irradiation condition at 10^6 R/h, the applicability of conventional perpendicular inspection probes is limited in the dose range of less than 1 x 10^8 rad due to the radiation damage of epoxy used for adhesion and filler material.

(2) The dose limit of conventional angular inspection probe with a acrylic wedge is 10^7 rad at 10^6 R/h.

(3) By optimizing the structure and material composition, two types of radiation-hard inspection probe, Type-A and Type-B, with wedge material of PEI and PI, were successfully developed. In the irradiation tests, both types showed the stable performance up to 10^9 rad and degradation of sensitivity was not observed.

(4) No serious irradiation damage on the characteristics of beam path length, refraction angle were found in testing of Type-A and Type-B.

(5) Regarding the characteristics on sensitivity, beam path length and refraction angle, no significant dependency on the wedge material was found in both types.

(6) On the peak frequency and band width of inspection frequency, Type-A which has a mechanically supported structure showed much stable performance than those of Type-B which has a modular structure.

Acknowledgments

The authors would like to express their sincere appreciation to Drs. M. Ohta, M. Seki, T. Tsunematsu, S. Matsuda and S. Shimamoto for their continuous guidance and encouragement on this work. They also would like to Toshiba Co. who are cooperated in this development.

Reference

[1] K. Obara, et al., "Irradiation Tests of Critical Components for Remote Handling System in Gamma Radiation Environment", JAERI-Tech 96-011, February (1996)

4. Conclusion

Based on the results obtained by the irradiation test of conventional ultrasonic inspection probes at 10^6 R/h, two types of radiation-hard probe, Type-A and Type-B, have been successfully developed. The characteristics of these radiation-hard probes were measured in normal and gamma-ray irradiation conditions. Through the series of testing on conventional and newly developed radiation-hard ultrasonic probes, the following conclusion were obtained;

(1) In the gamma ray irradiation condition at 10^6 R/h, the applicability of conventional perpendicular inspection probes is limited in the dose range of less than 1 x 10^8 rad due to the radiation damage of epoxy used for adhesion and filler material.

(2) The dose limit of conventional angular inspection probe with a acrylic wedge is 10^7 rad at 10^6 R/h.

(3) By optimizing the structure and material composition, two types of radiation-hard inspection probe, Type-A and Type-B, with wedge material of PEI and PI, were successfully developed. In the irradiation tests, both types showed the stable performance up to 10^9 rad and degradation of sensitivity was not observed.

(4) No serious irradiation damage on the characteristics of beam path length, refraction angle were found in testing of Type-A and Type-B.

(5) Regarding the characteristics on sensitivity, beam path length and refraction angle, no significant dependency on the wedge material was found in both types.

(6) On the peak frequency and band width of inspection frequency, Type-A which has a mechanically supported structure showed much stable performance than those of Type-B which has a modular structure.

Acknowledgments

The authors would like to express their sincere appreciation to Drs. M. Ohta, M. Seki, T. Tsunematsu, S. Matsuda and S. Shimamoto for their continuous guidance and encouragement on this work. They also would like to Toshiba Co. who are cooperated in this development.

Reference

[1] K. Obara, et al., "Irradiation Tests of Critical Components for Remote Handling System in Gamma Radiation Environment", JAERI-Tech 96-011, February (1996)

4. Conclusion

Based on the results obtained by the irradiation test of conventional ultrasonic inspection probes at 10^6 R/h, two types of radiation-hard probe, Type-A and Type-B, have been successfully developed. The characteristics of these radiation-hard probes were measured in normal and gamma-ray irradiation conditions. Through the series of testing on conventional and newly developed radiation-hard ultrasonic probes, the following conclusion were obtained;

(1) In the gamma ray irradiation condition at 10^6 R/h, the applicability of conventional perpendicular inspection probes is limited in the dose range of less than 1 x 10^8 rad due to the radiation damage of epoxy used for adhesion and filler material.

(2) The dose limit of conventional angular inspection probe with a acrylic wedge is 10^7 rad at 10^6 R/h.

(3) By optimizing the structure and material composition, two types of radiation-hard inspection probe, Type-A and Type-B, with wedge material of PEI and PI, were successfully developed. In the irradiation tests, both types showed the stable performance up to 10^9 rad and degradation of sensitivity was not observed.

(4) No serious irradiation damage on the characteristics of beam path length, refraction angle were found in testing of Type-A and Type-B.

(5) Regarding the characteristics on sensitivity, beam path length and refraction angle, no significant dependency on the wedge material was found in both types.

(6) On the peak frequency and band width of inspection frequency, Type-A which has a mechanically supported structure showed much stable performance than those of Type-B which has a modular structure.

Acknowledgments

The authors would like to express their sincere appreciation to Drs. M. Ohta, M. Seki, T. Tsunematsu, S. Matsuda and S. Shimamoto for their continuous guidance and encouragement on this work. They also would like to Toshiba Co. who are cooperated in this development.

Reference

[1] K. Obara, et al., "Irradiation Tests of Critical Components for Remote Handling System in Gamma Radiation Environment", JAERI-Tech 96-011, February (1996)

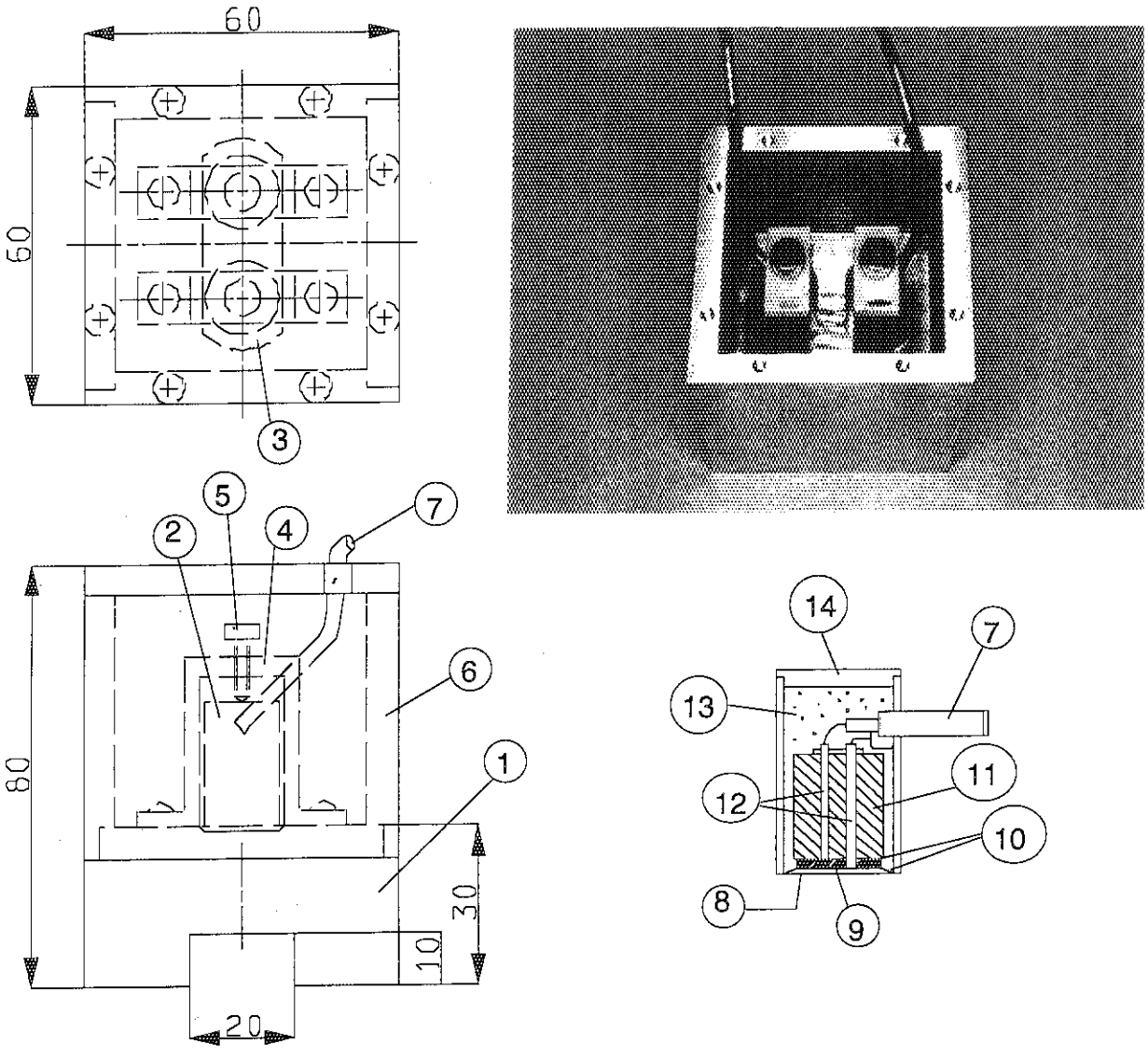

1: Test sample
2: UT probe
3: Slit
4: Probe guide
5: Holding screw
6: Frame
7: Cable
8: Protector (Al2O3)
9: Wave source ($PbNb_2O_6$)
10: Adhesive (Epoxy resin)
11: Dumper (powdered W in epoxy)
12: Conductor (Cu)
13: Filler (Epoxy)
14: Casing (SS304)

Fig. 2.1 Configuration of perpendicular type UT inspection probe employed for gamma ray irradiation test

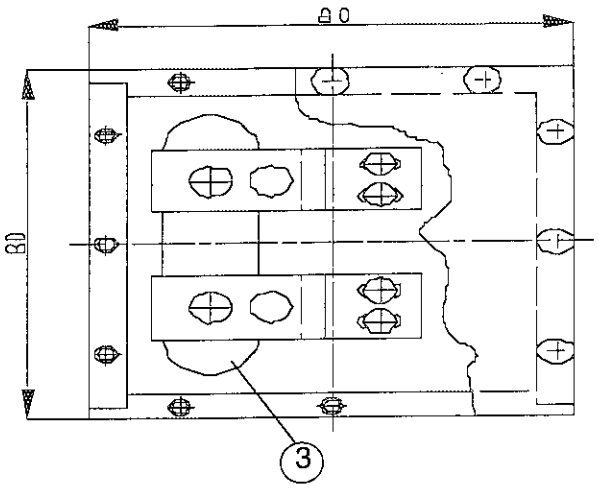

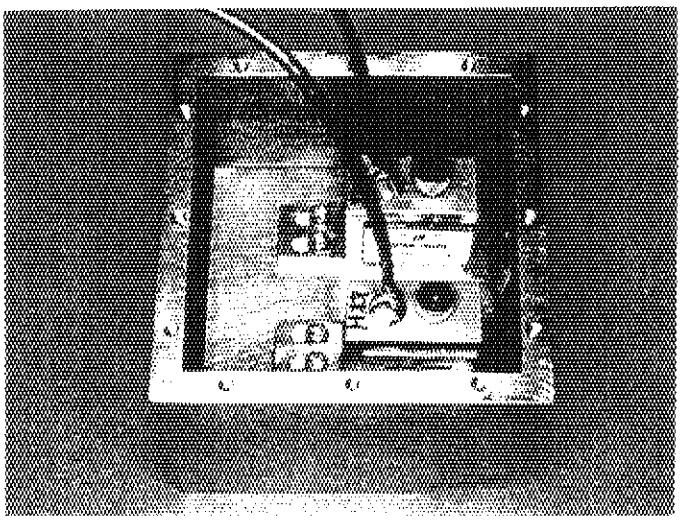

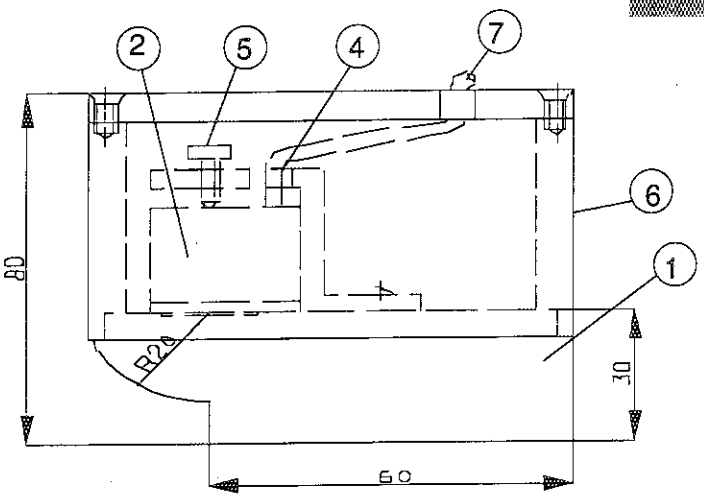

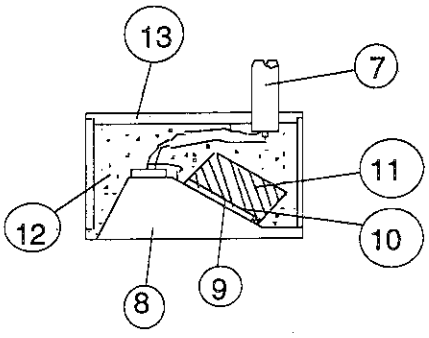

1: Test piece
2: UT probe
3: Slit
4: Probe guide
5: Holding screw
6: Frame
7: Cable
8: Wedge (Acryl, PEI)
9: Wave source ($PbNb_2O_6$)
10: Adhesive (Epoxy resin)
11: Dumper (powdered W in epoxy)
12: Filler (Epoxy)
13: Casing (SS304)

Fig. 2.2 Configuration of angular type UT inspection probe employed for gamma ray irradiation test

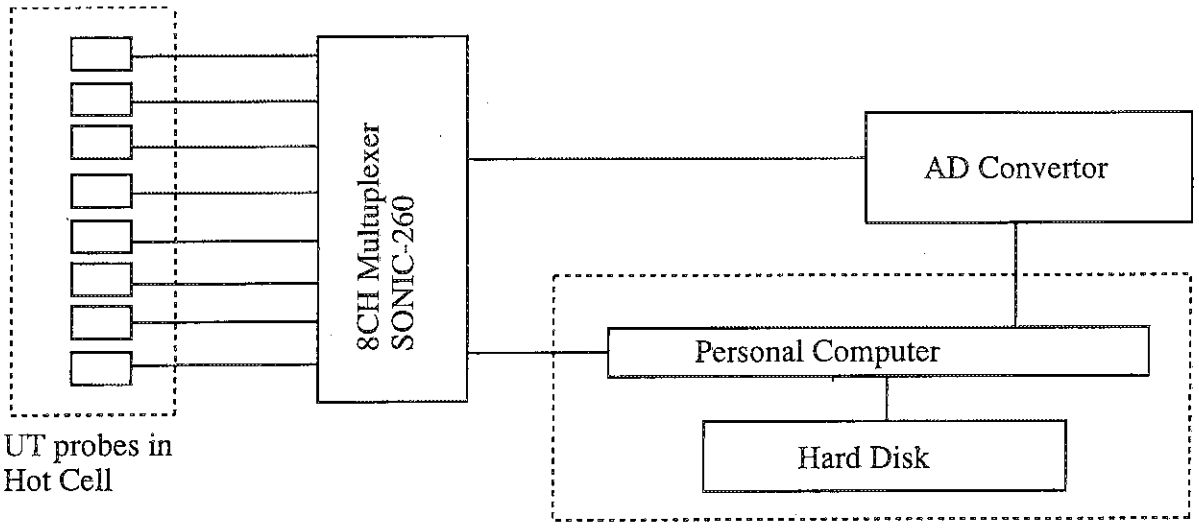

Fig. 2.3 Data acquisition system for the irradiation test of ultrasonic inspection probes

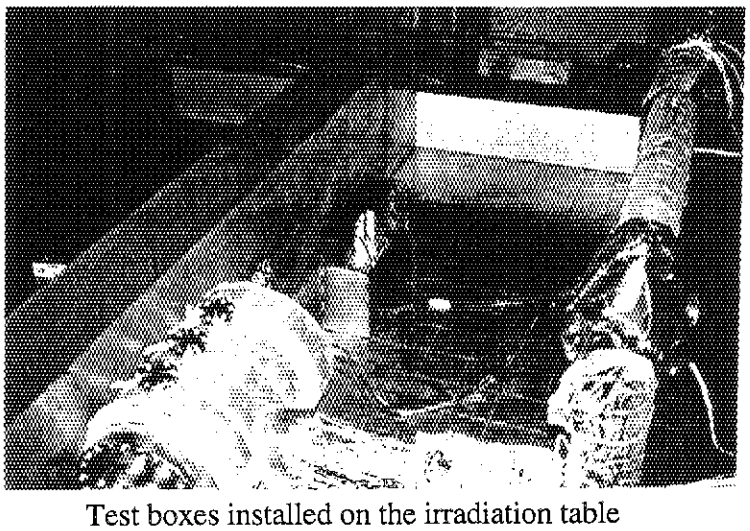

Test boxes installed on the irradiation table

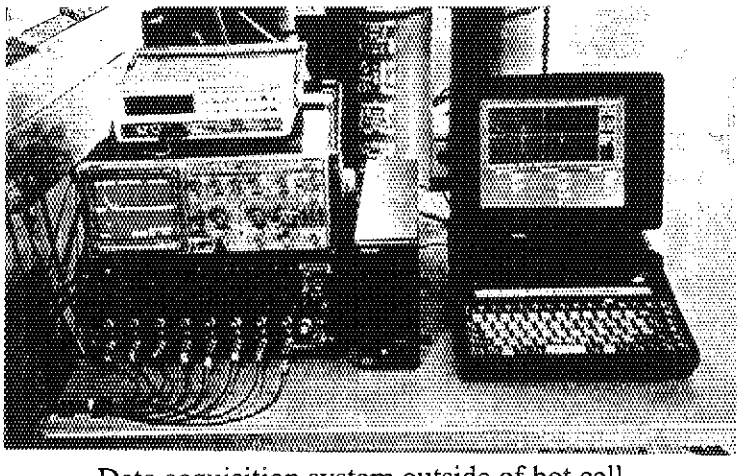

Data acquisition system outside of hot cell

Fig. 2.4 Picture of test boxes installed on the irradiation table of ^{60}Co irradiation test facility and the data acquisition system outside of hot cell

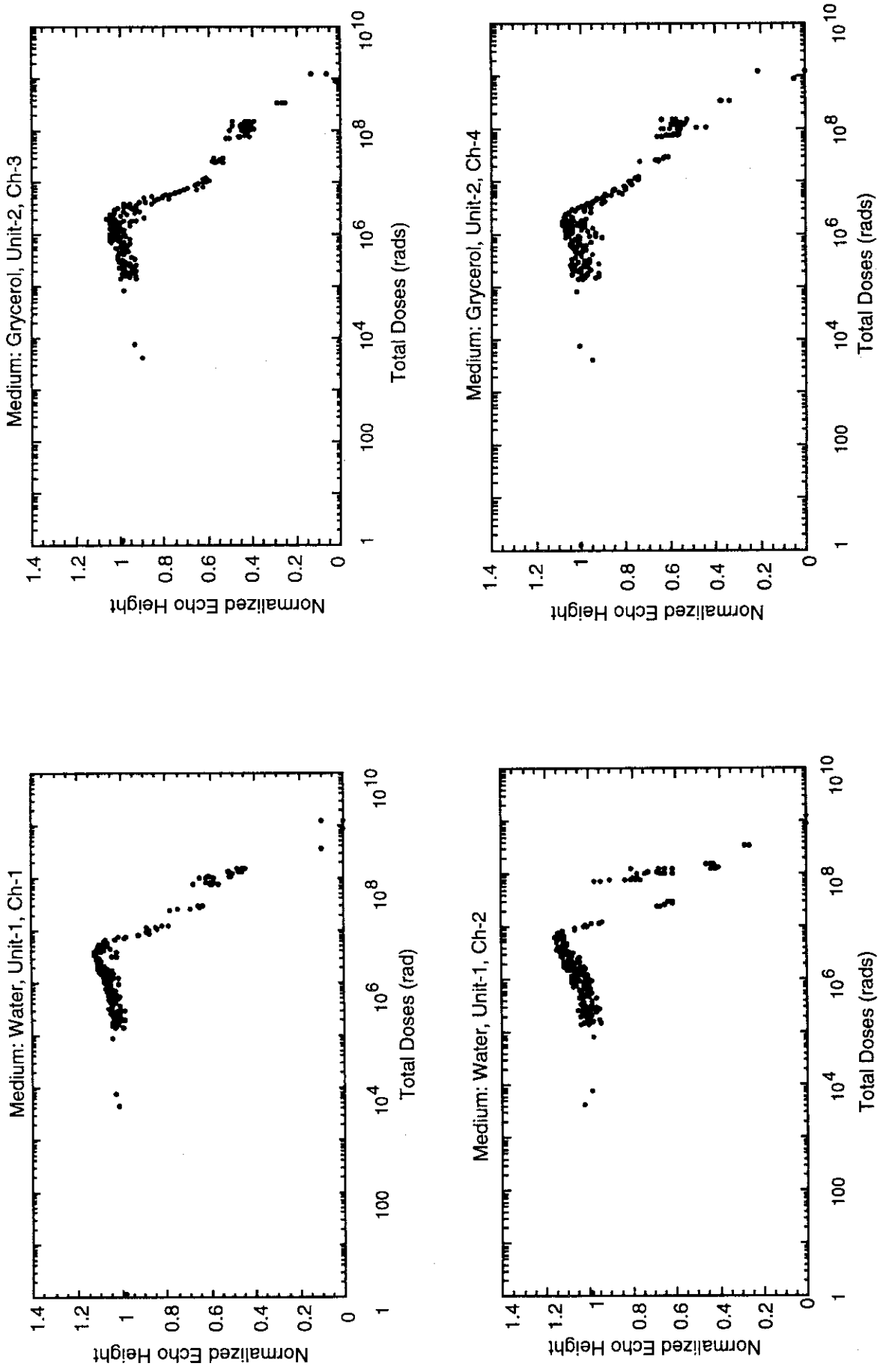

Fig. 2. 5 Change of echo height measured in the irradiation test of perpendicular UT inspection probes

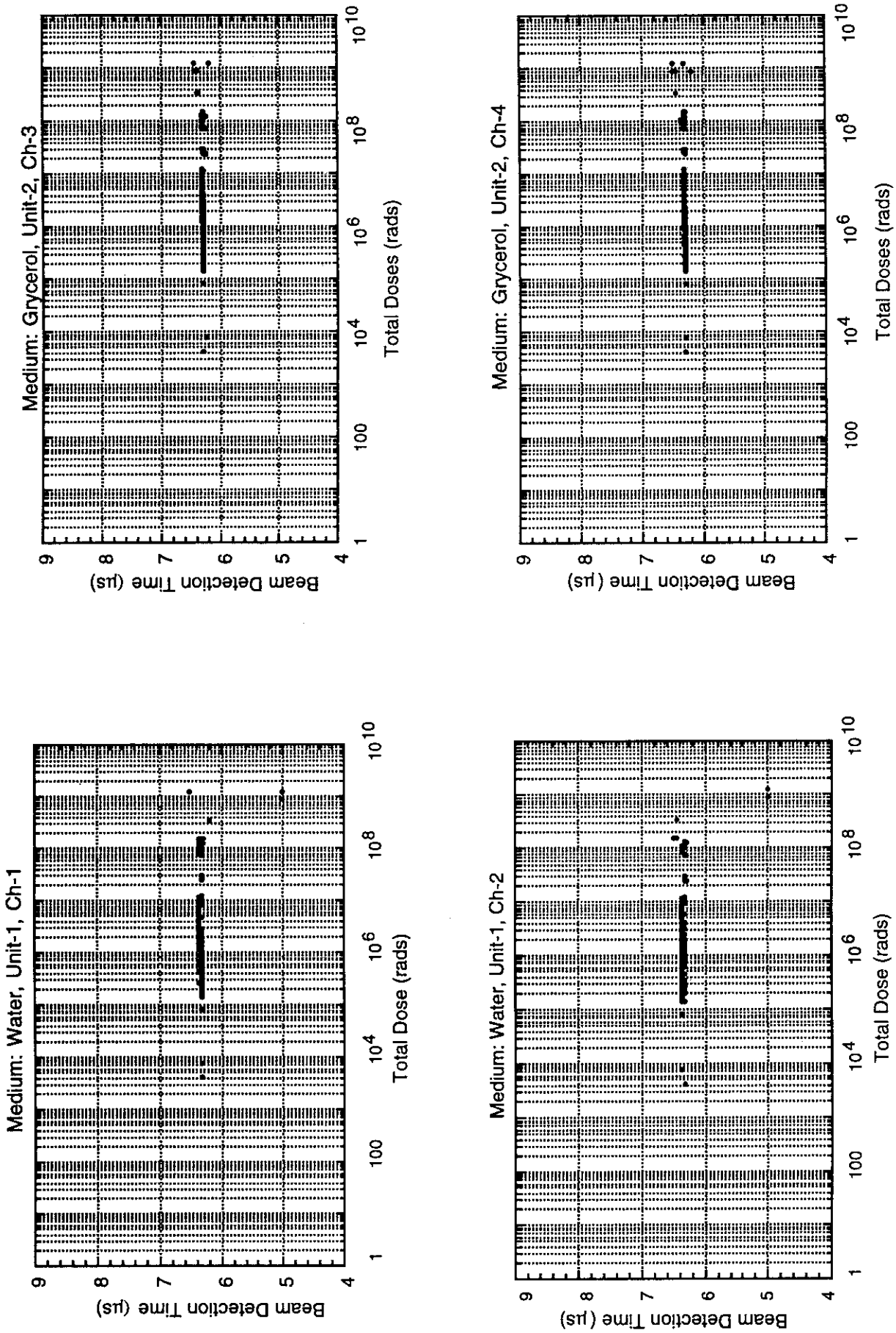

Fig. 2.6 Change of beam detection time measured in the irradiation test of perpendicular UT inspection probes

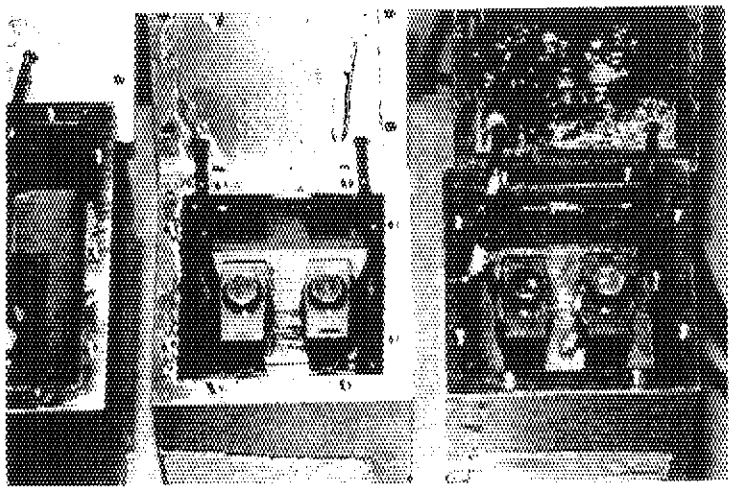

View of the inside of test boxes after the irradiation test up to 10^9 rad
Left: Medium - glycerol
Right: Medium - water

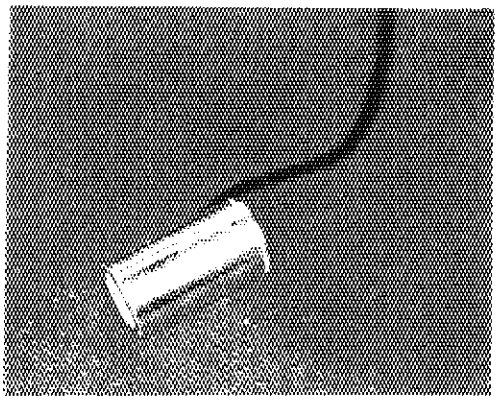

UT probe after the irradiation
Medium : glycerol

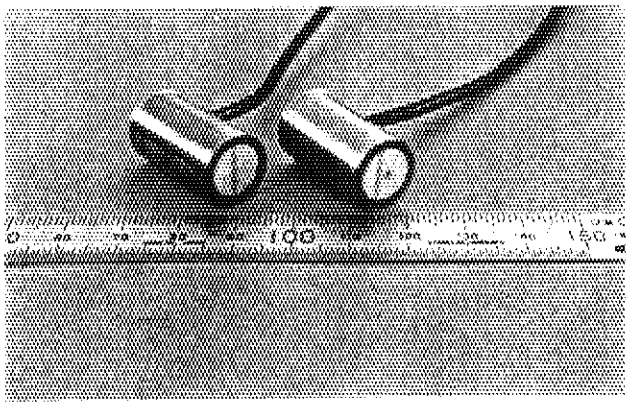

UT inspection probes before
the irradiation

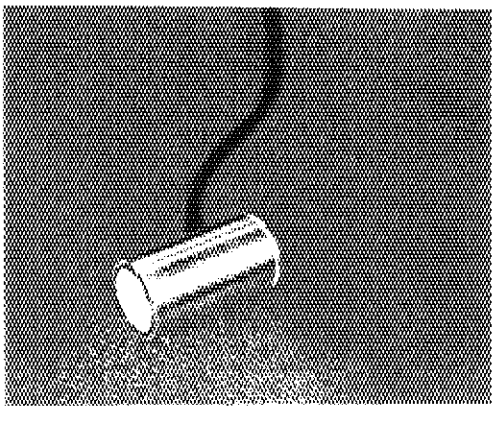

UT probe after the irradiation
Medium : water

Fig. 2.7 View of the perpendicular inspection probes after gamma ray irradiation test up to 10^9 rad

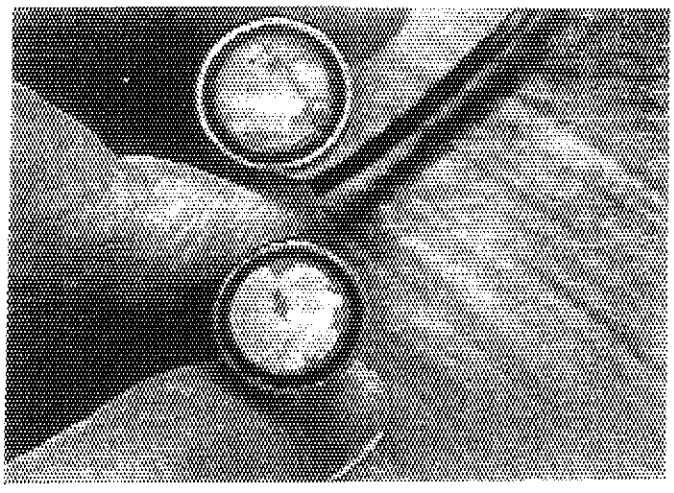

a) view of the oscillator after the removal of protector
- a part of bonded surface was broken due to the radiation damage of epoxy adhesive

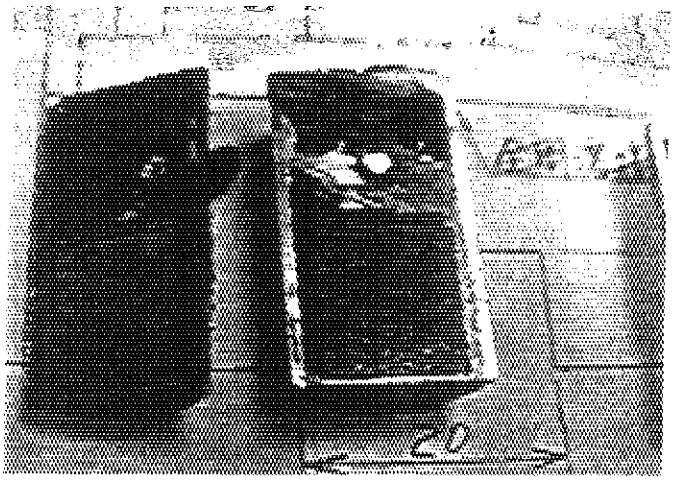

Crack

b) cross section of the probe after the cutting of casing
- crack was found between the damper and epoxy filler due to the swelling of epoxy

Fig. 2.8 **Cross-sectional view of perpendicular inspection probe after the irradiation test up to 10^9 rad**

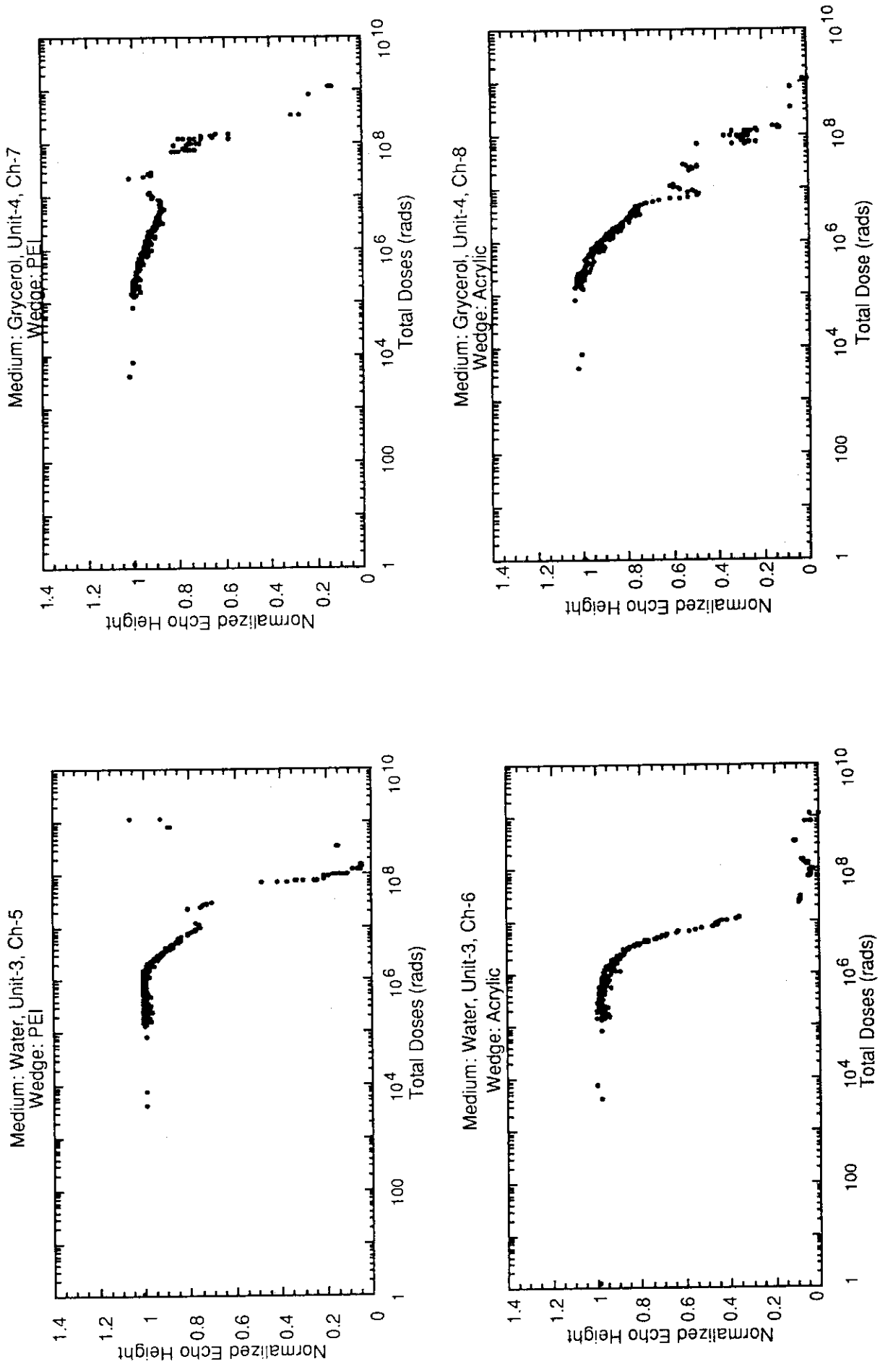

Fig. 2. 9 Change of echo height measured in the irradiation test of angular UT inspection probes

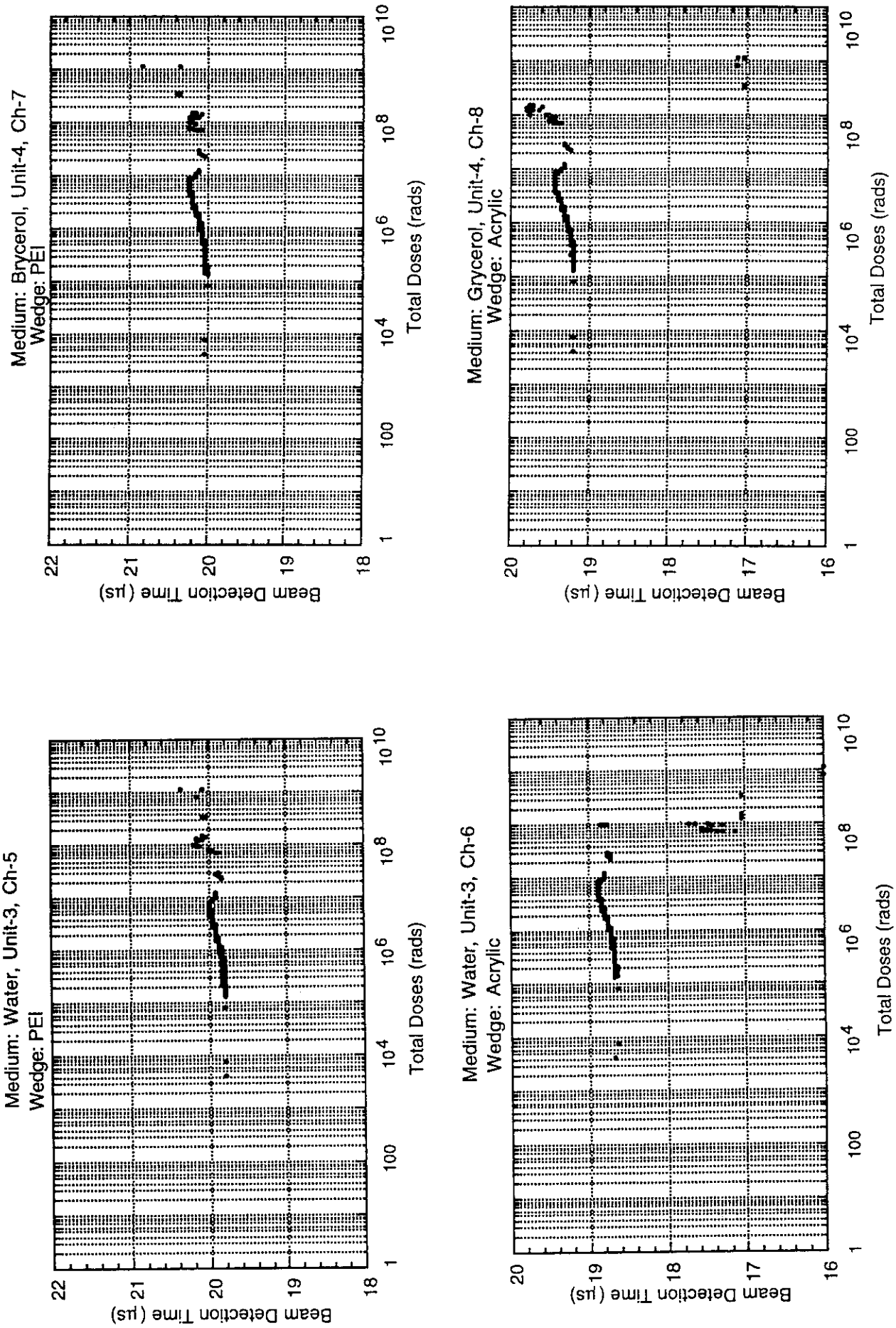

Fig. 2.10 Change of beam detection time measured in the irradiation test of angular UT inspection probes

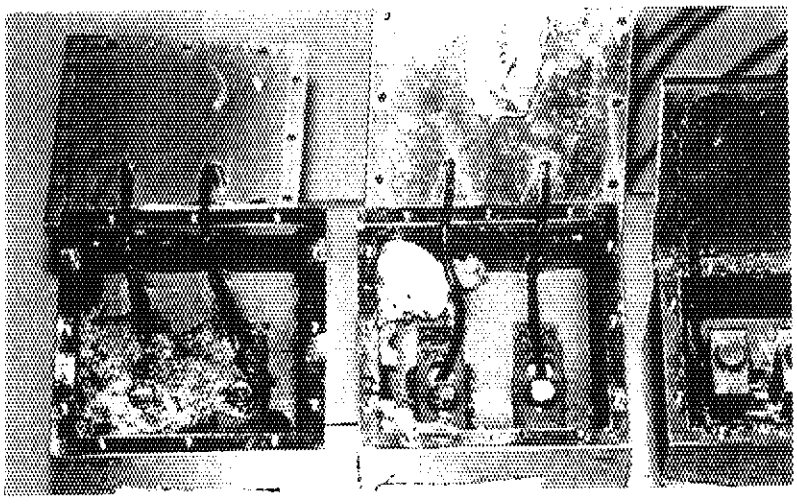

View of the inside of test boxes after the irradiation test up to 10^9 rad
Left: Medium - glycerol
Right: Medium - water

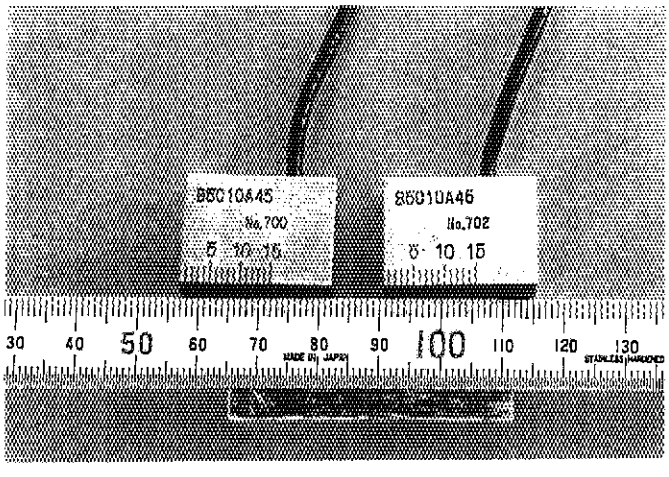

UT inspection probes before the irradiation

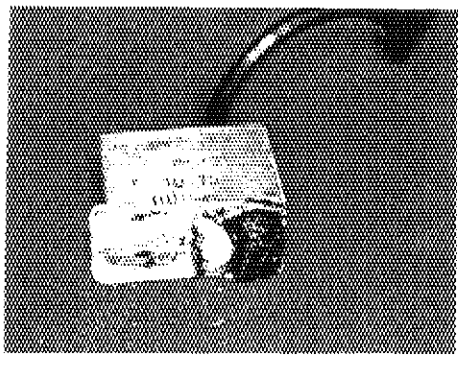

UT probe after the irradiation
Medium : water
Wedge: acrylic

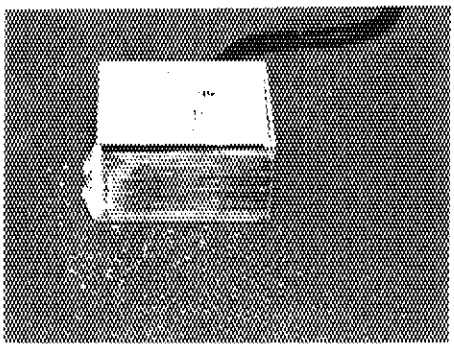

UT probe after the irradiation
Medium : water
Wedge: PEI

Fig. 2.11 View of the angular inspection probes after gamma ray irradiation test up to 10^9 rad

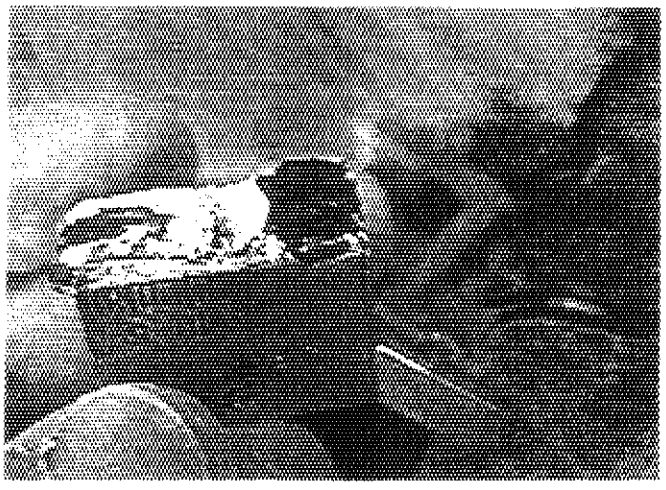

a) view of the probe after the gamma ray irradiation test
- Deformation of casing due to the swelling of epoxy filler was observed
- Almost all volume of acrylic wedge is disappeared due to decomposition

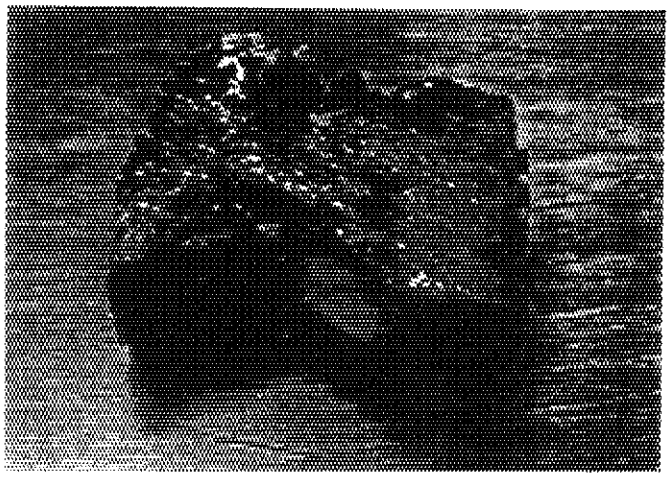

b) cross section of the probe after the cutting of casing
- No wedge material
- Reduction of filler volume
- Many porous structures were observed in epoxy filler due to the swelling of epoxy
- Crack in the oscillator

Fig. 2.12 **Cross-sectional view of angular inspection probe after the irradiation test up to 10^9 rad**
Wedge material : acrylic

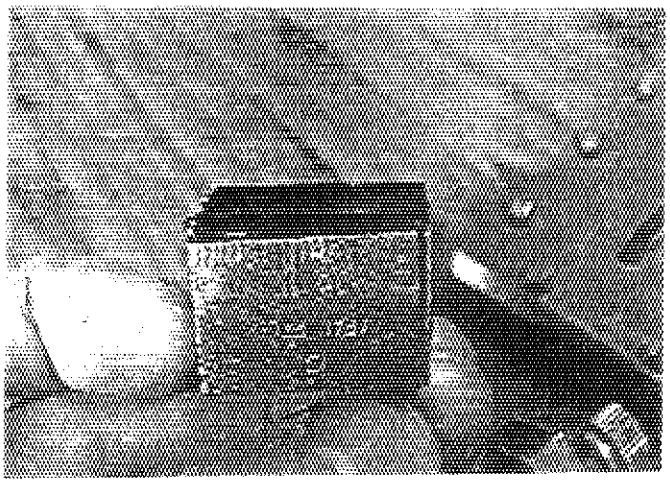

a) view of the probe after the gamma ray irradiation test
   - Deformation of casing due to the swelling of epoxy filler was observed

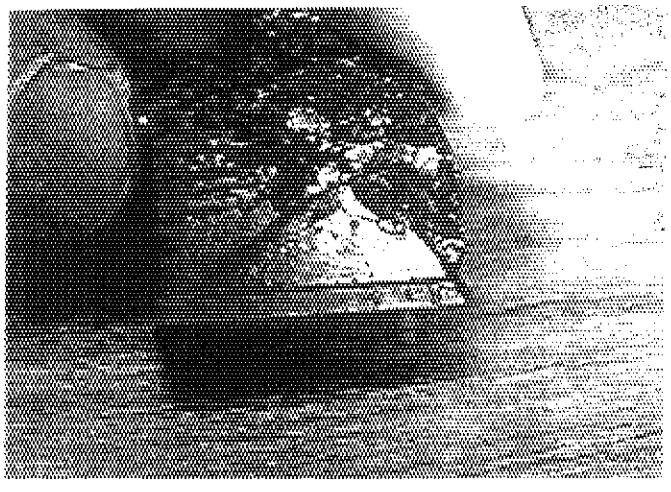

b) cross section of the probe after the cutting of casing
   - No damage in wedge material
   - Many porous structures were observed in epoxy filler due to the swelling of epoxy

Fig. 2.13 **Cross-sectional view of angular inspection probe after the irradiation test up to 10^9 rad**
Wedge material : PEI

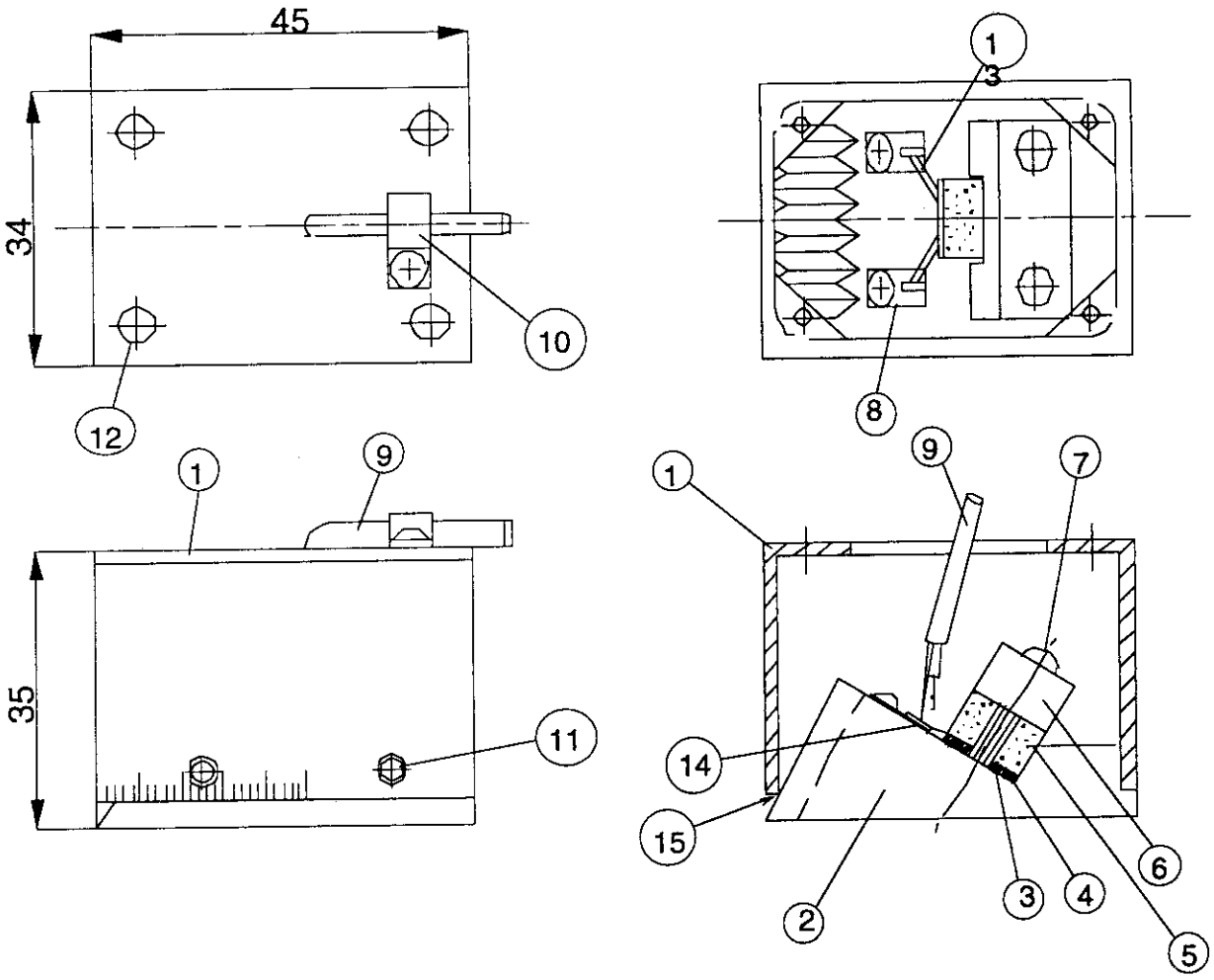

1: Casing (SS304)
2: Wedge (PEI, PI)
3: Adhesive (Epoxy)
4: Wave source ($PbNb_2O_6$)
5: Damper (powdered W in epoxy)
6: Probe holder (PI)
7: Holding screw
8: Base (FRP)
9: Cable
10: Cable holder
11: Holding screw
12: Holding screw
13: Conductor (Cu)
14: Solder
15: Sealing (Epoxy)

Fig. 3.1 Configuration of radiation hard ultra-sonic inspection probe (angular type-A)
- No epoxy filler
- No adhesion between wave source and dumper
- Wavy-shaped dumper to reduce noise signal
- Minimum use of epoxy resin

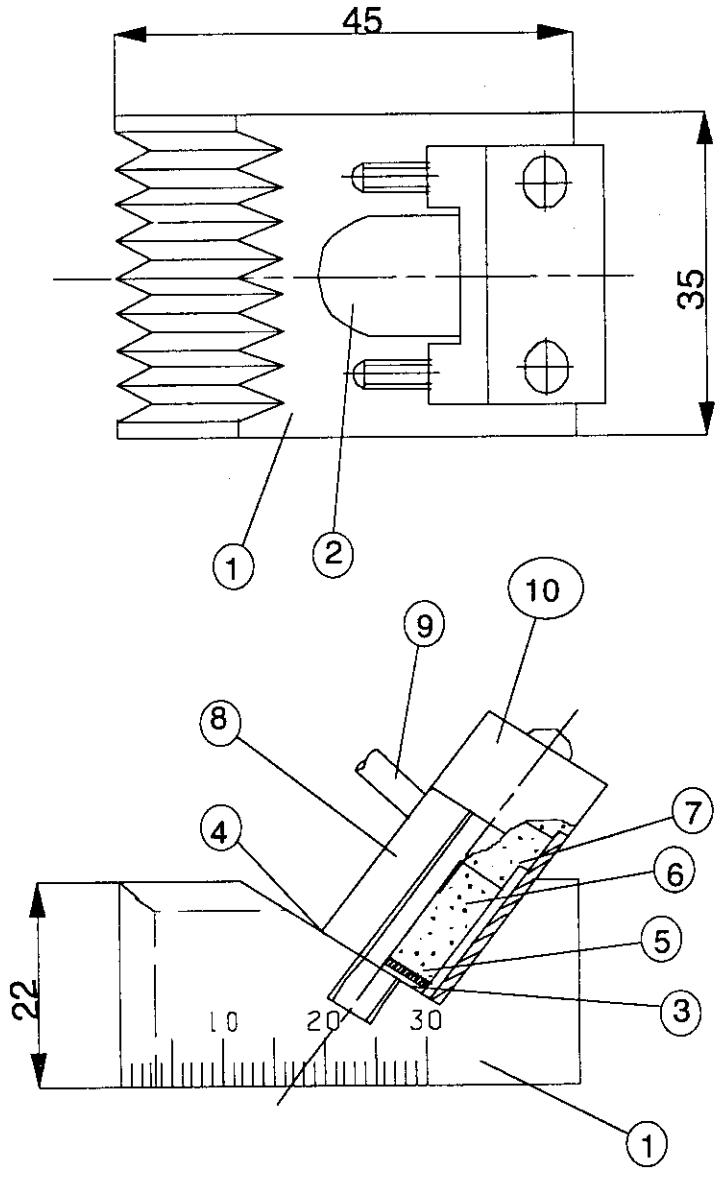

1: Wedge (PEI, PI)
2: UT probe
3: Protector (Epoxy)
4: Couplant
5: Wave source (PbNb2O6)
6: Damper (powdered W in epoxy)
7: Filler (Epoxy)
8: Casing (SS304)
9: Cable
10: Holder (SS304)

Fig. 3.2 Configuration of radiation hard ultra-sonic inspection probe (angular type-B)
- High mechanical integrity with modular structure
- Epoxy filler for high temperature use
- Wavy-shaped dumper to reduce noise signal
- Minimum use of epoxy resin

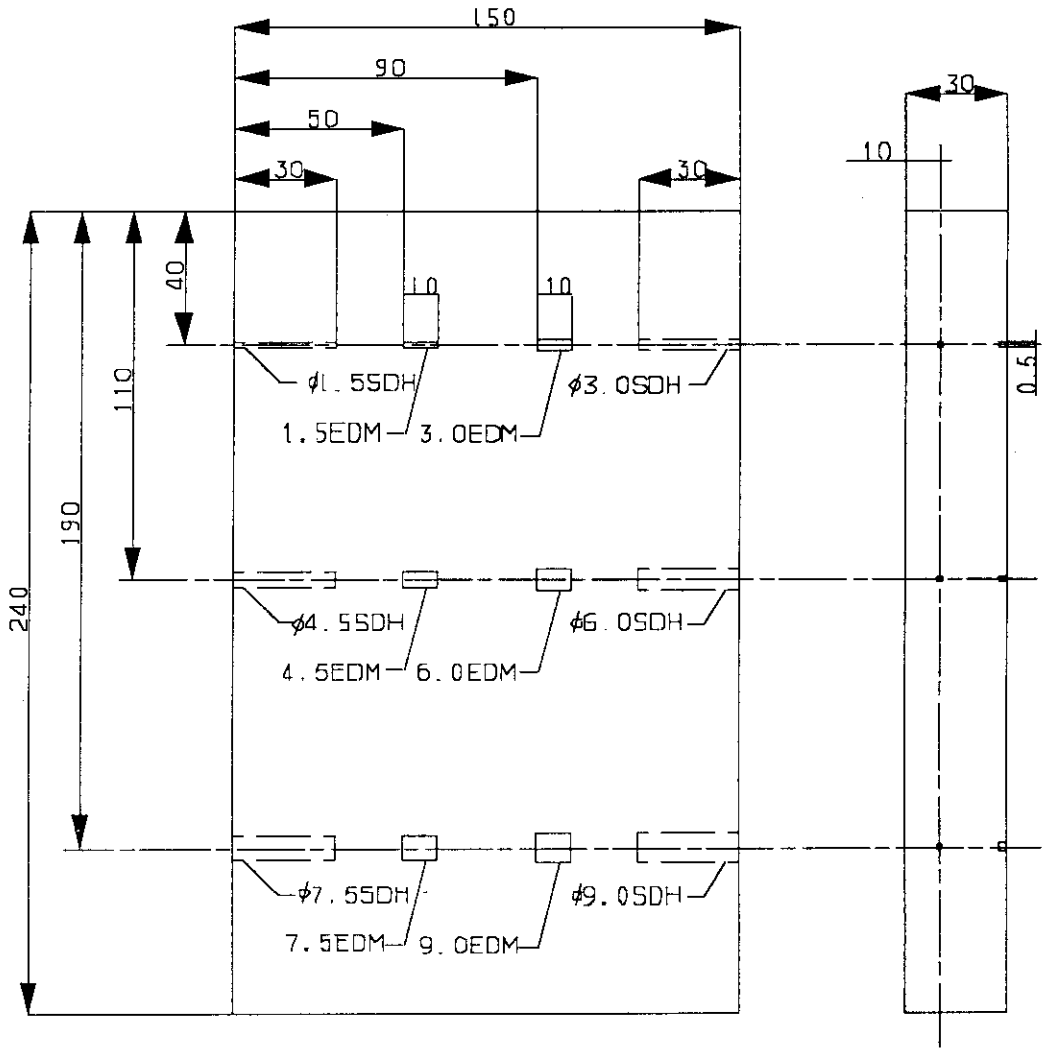

Fig. 3.3 Test samples with artificial defects for the evaluation of sensitivity

- **Material : SS316 and Inconel 625**
- **Plate thickness: 30 mm**
- **Flaw type: side drill hole (SDH) and slit machined by electrical discharge machining (EDM)**
- **Defect size: SDH: 1.5 mmΦ,3.0 mmΦ, 6.0 mmΦ and 9.0 mmΦ**
  EDM: 1.5 mm,3.0 mm, 6.0 mm and 9.0 mmf

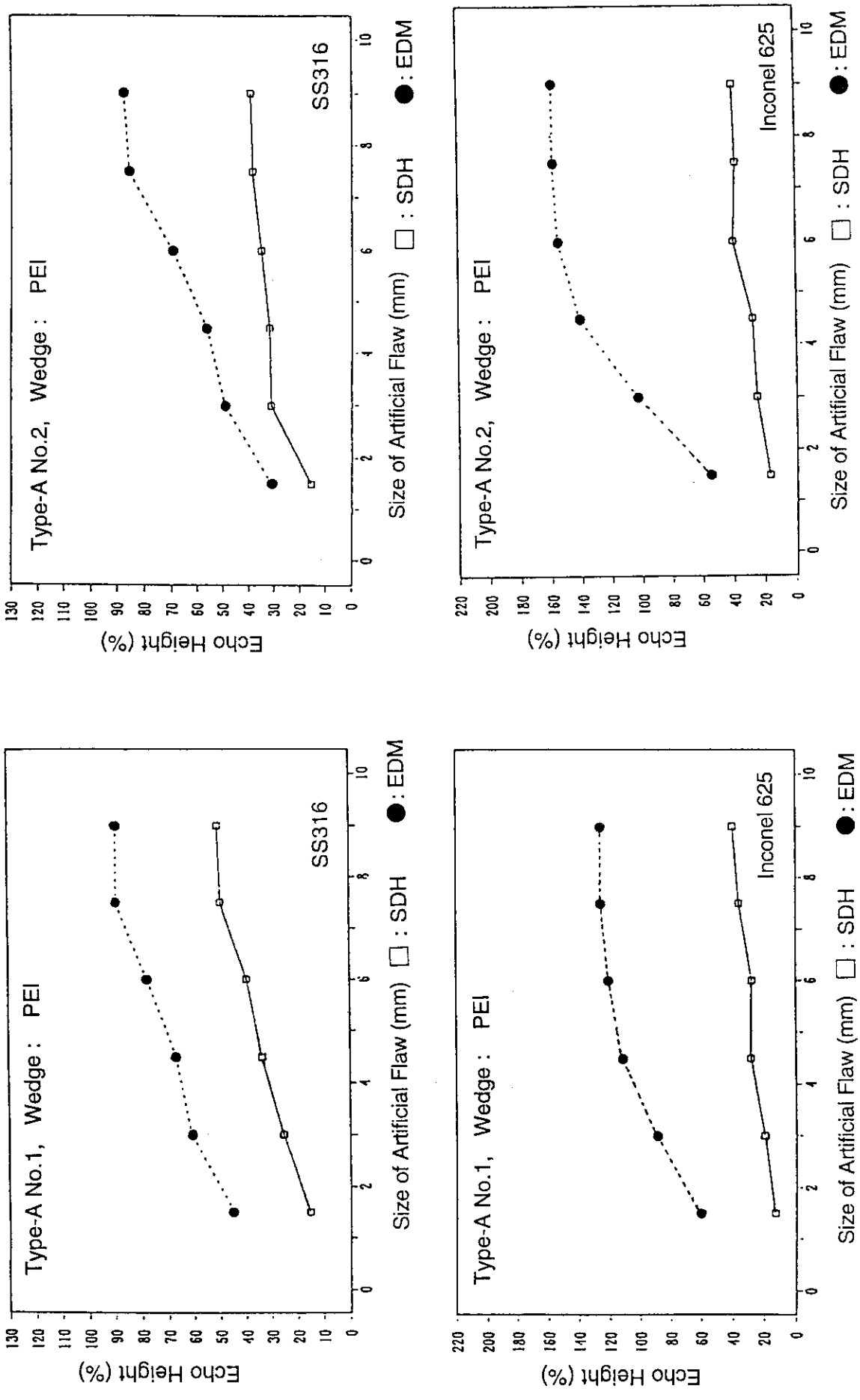

Fig. 3.4 The sensitivity of the angular probe Type-A to the various size of flaw (1)
SDH: side drill hole, EDM: slit machined by electrical discharge

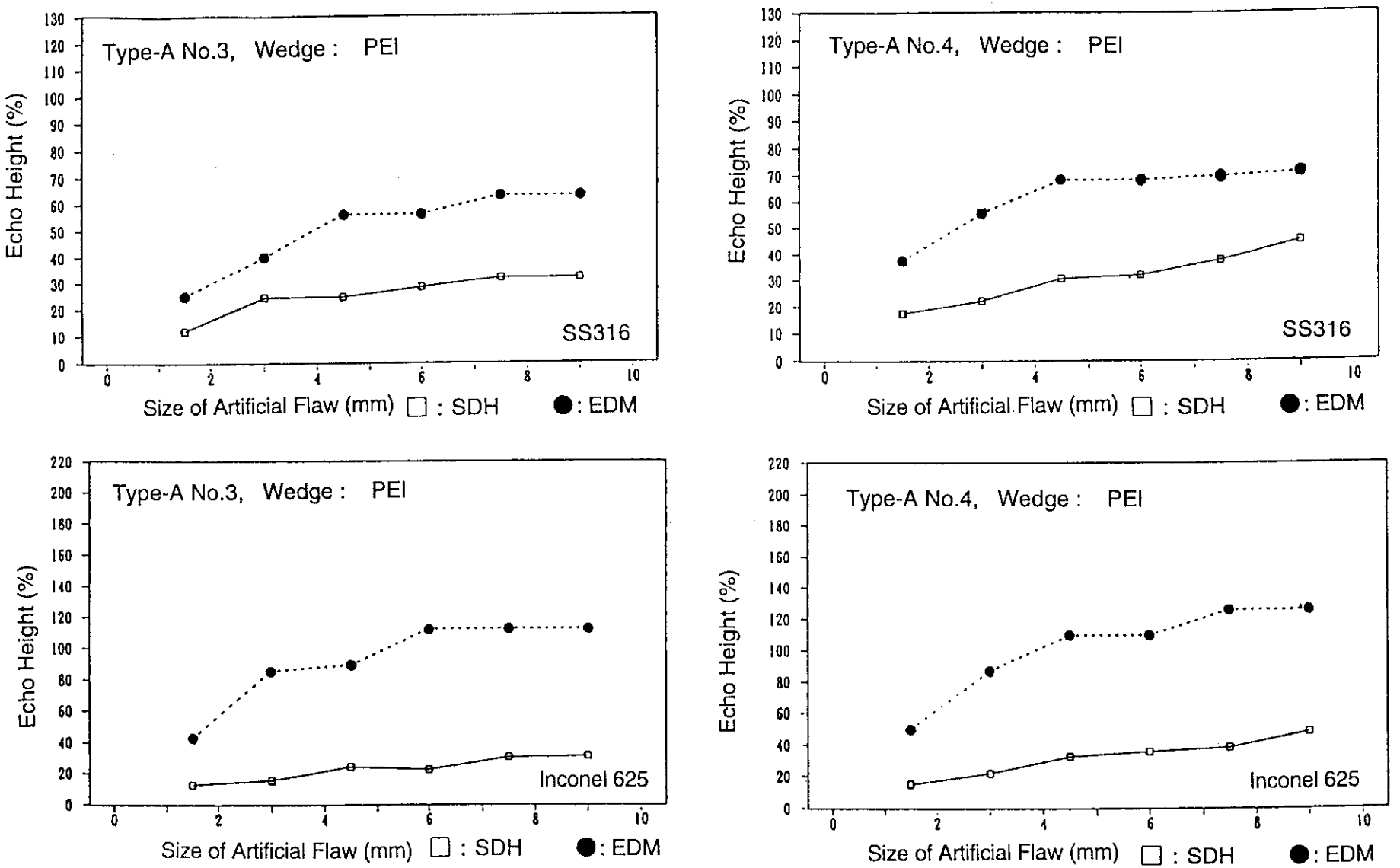

Fig. 3.5 The sensitivity of the angular probe Type-A to the various size of flaw (2)
SDH: side drill hole, EDM: slit machined by electrical discharge

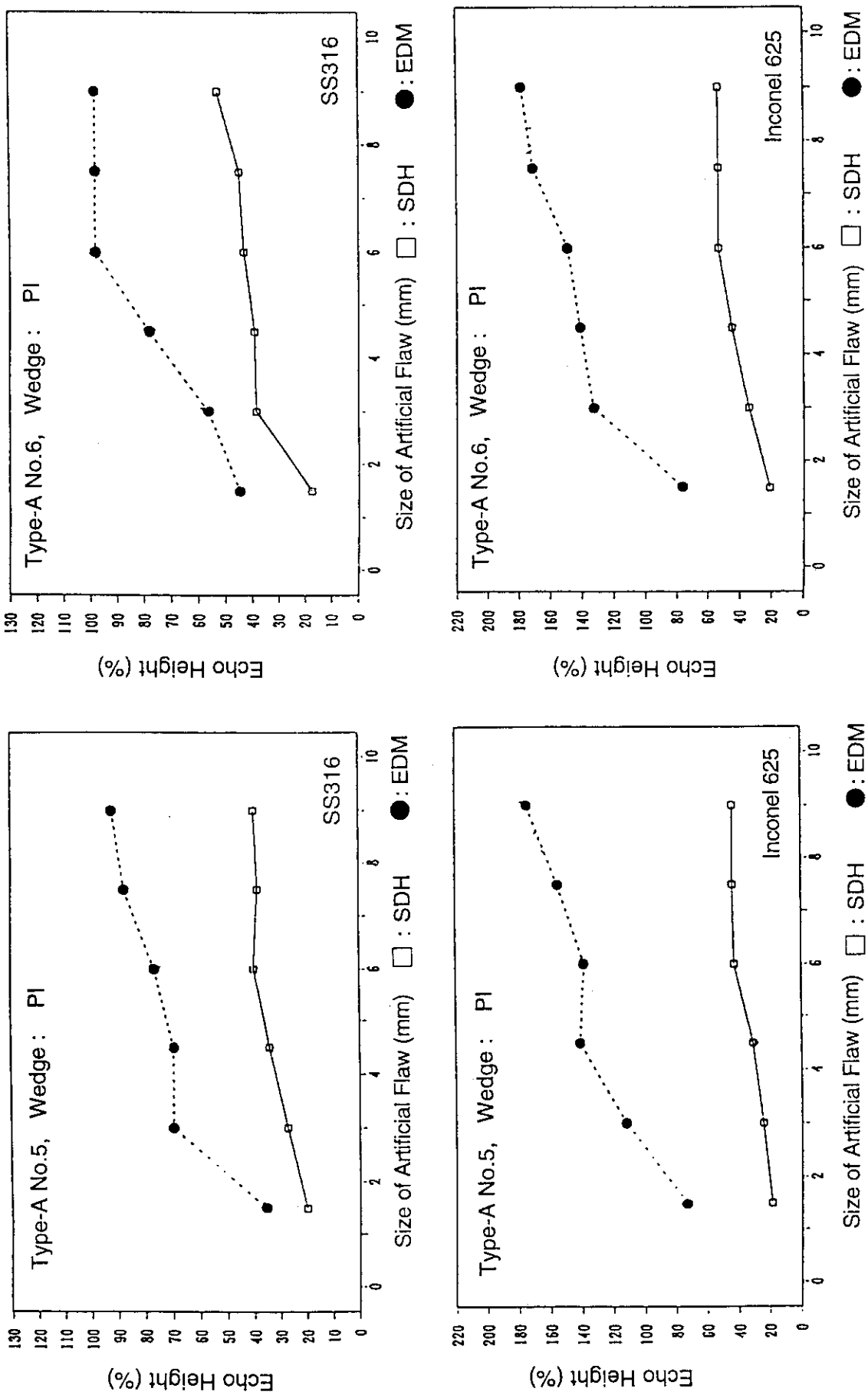

Fig. 3.6 The sensitivity of the angular probe Type-A to the various size of flaw (3)
SDH: side drill hole, EDM: slit machined by electrical discharge

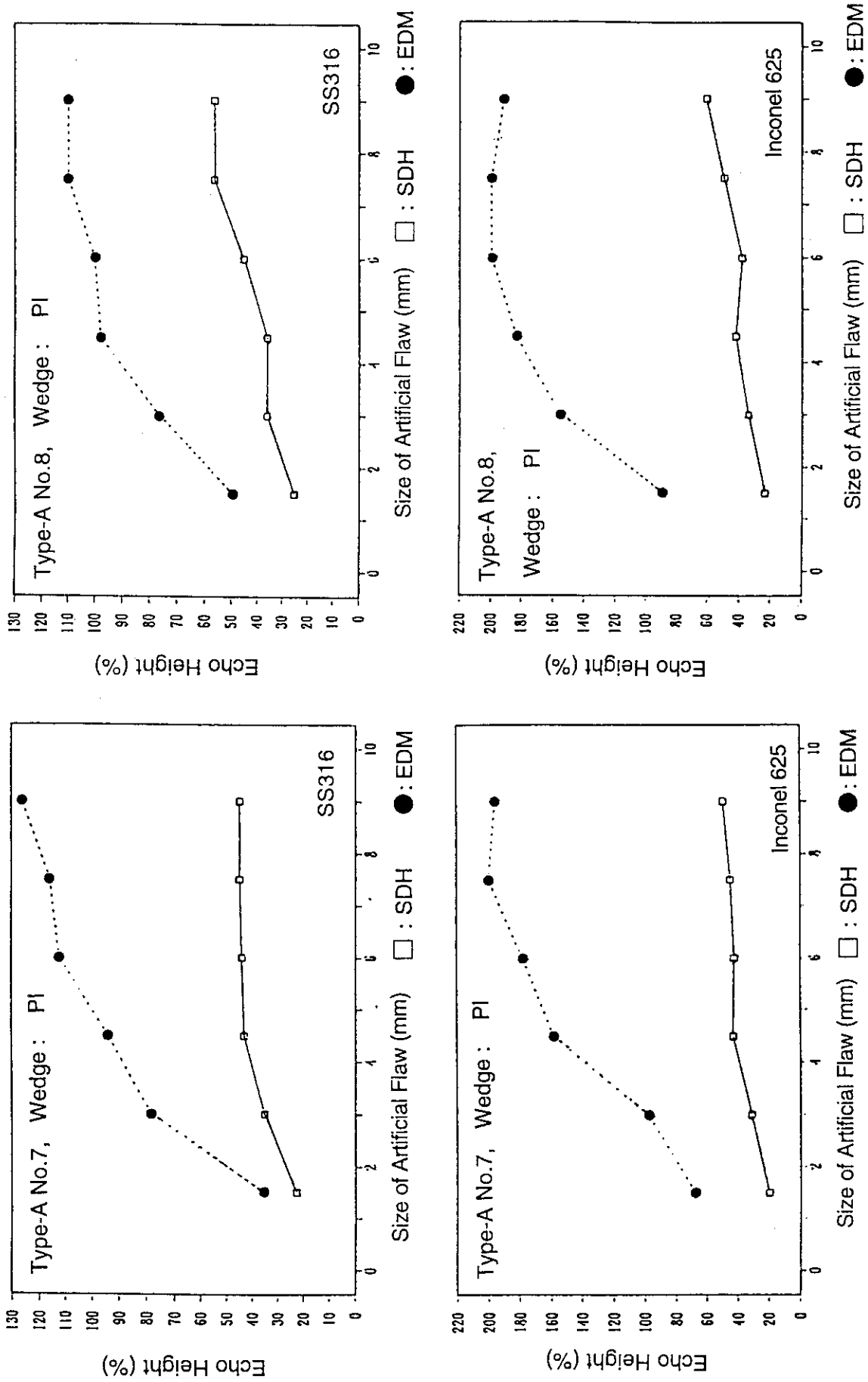

Fig. 3.7 The sensitivity of the angular probe Type-A to the various size of flaw (4)
SDH: side drill hole, EDM: slit machined by electrical discharge

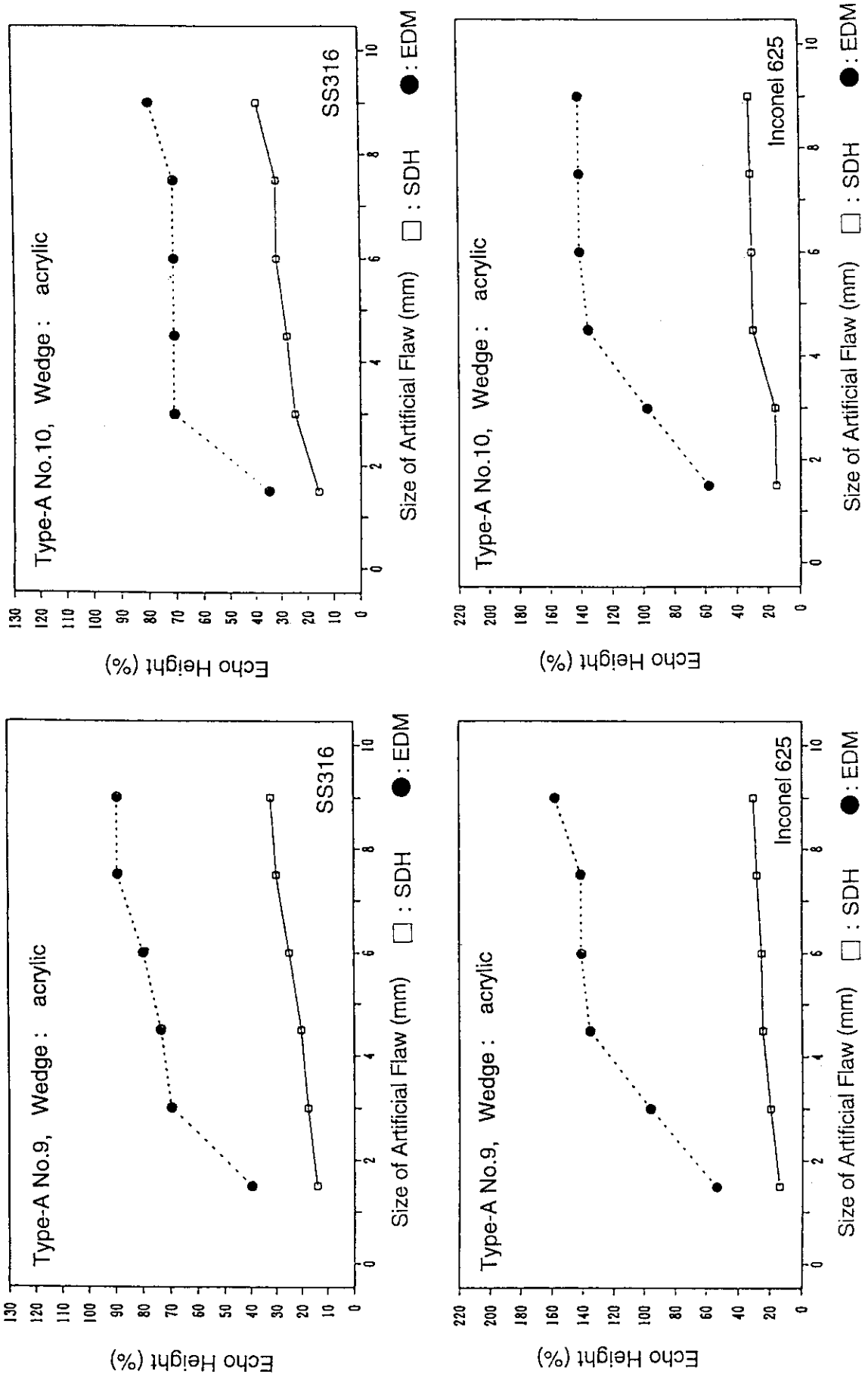

Fig. 3.8 The sensitivity of the angular probe Type-A to the various size of flaw (5)
SDH: side drill hole, EDM: slit machined by electrical discharge

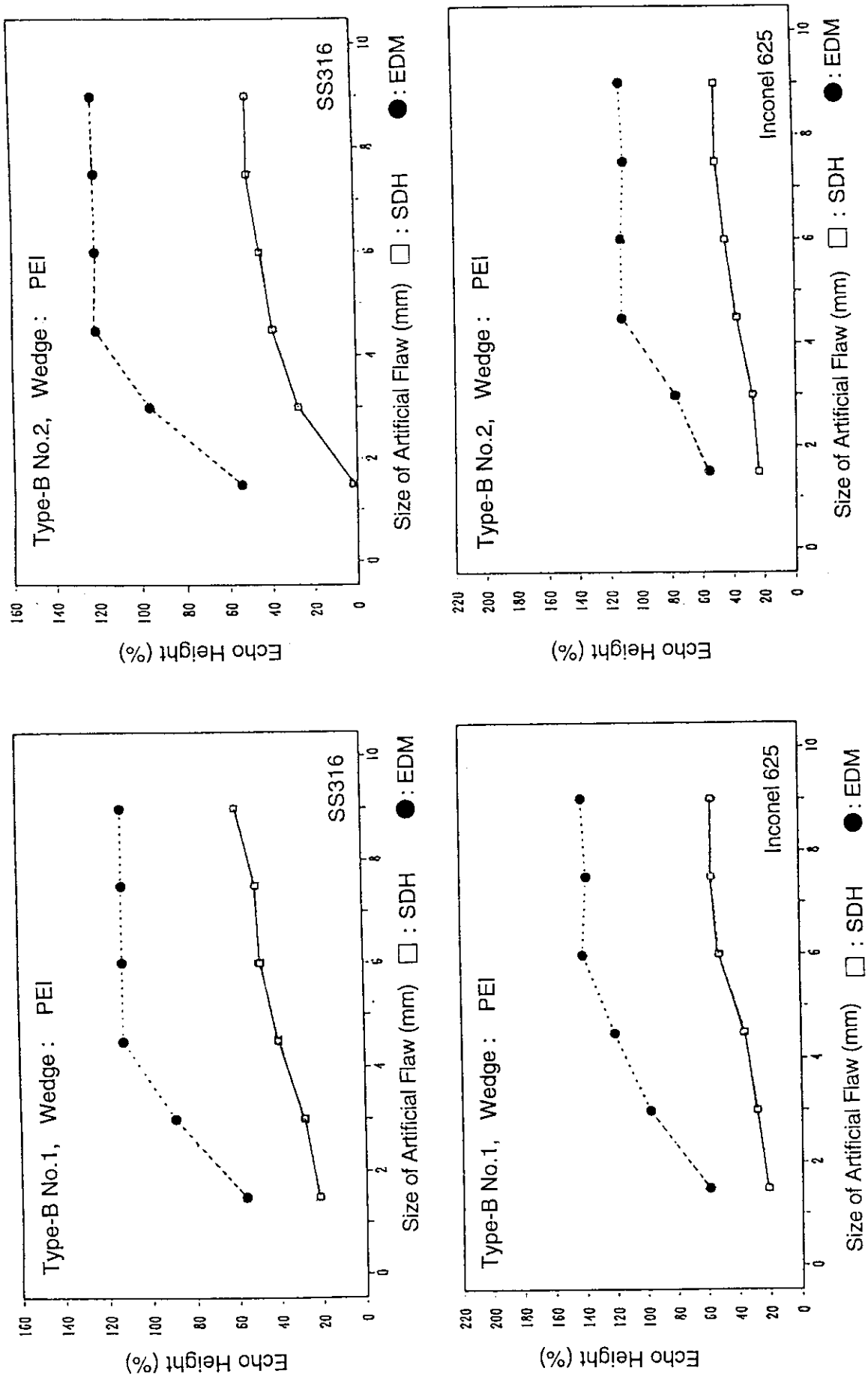

Fig. 3.9 The sensitivity of the angular probe Type-B to the various size of flaw (1)
SDH: side drill hole, EDM: slit machined by electrical discharge

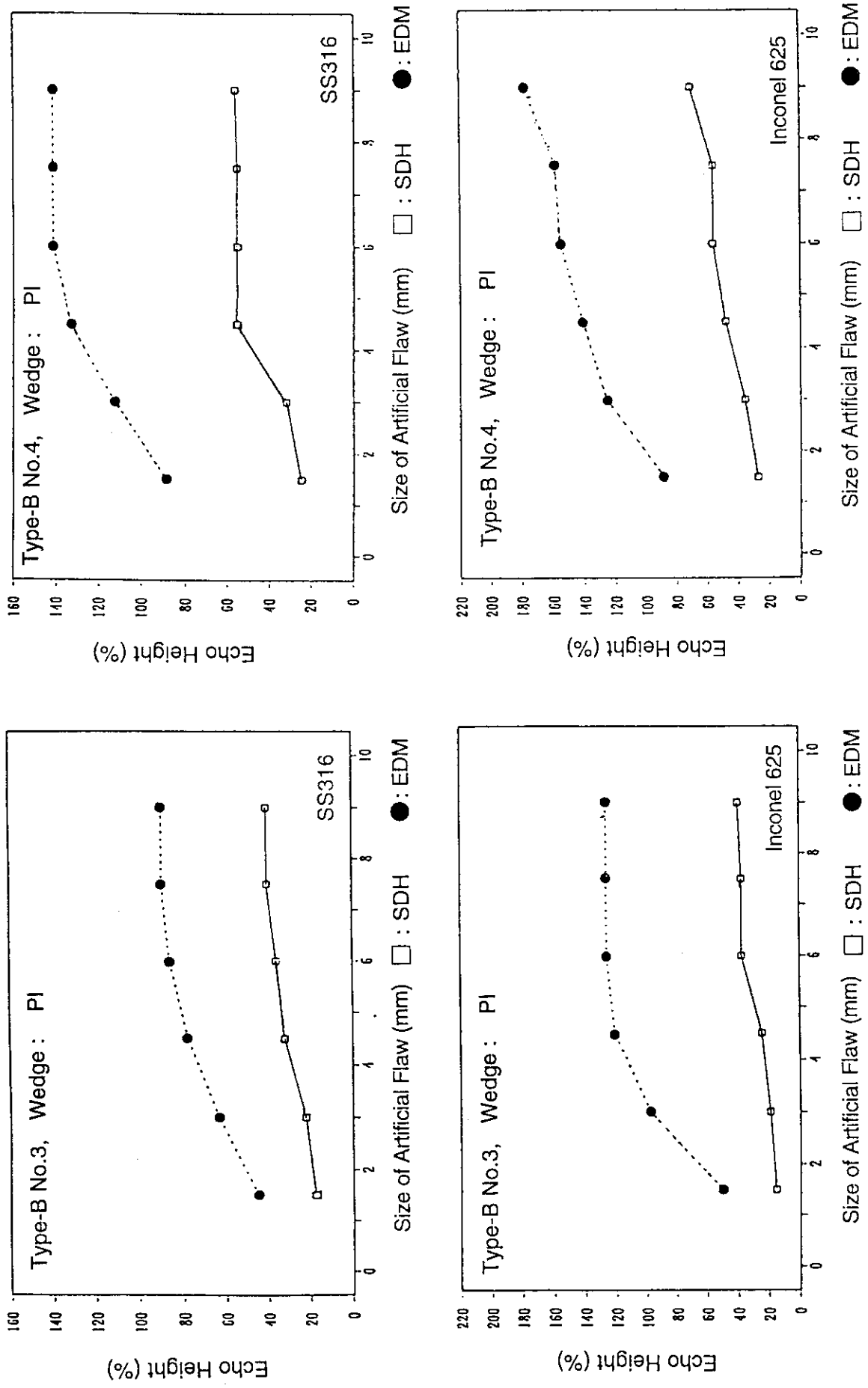

Fig. 3.10 The sensitivity of the angular probe Type-B to the various size of flaw (2)
SDH: side drill hole, EDM: slit machined by electrical discharge

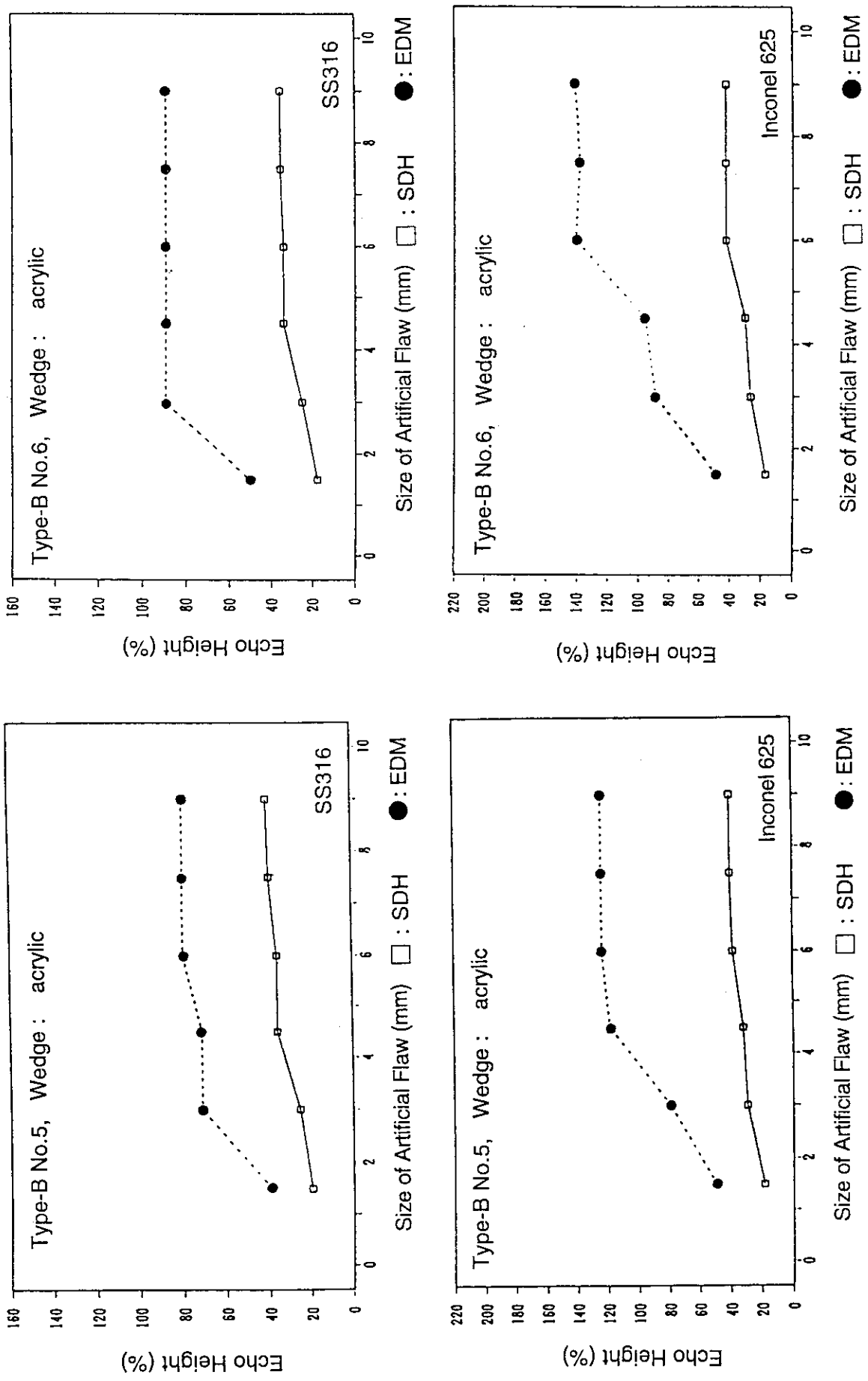

Fig. 3.11 The sensitivity of the angular probe Type-B to the various size of flaw (3)
SDH: side drill hole, EDM: slit machined by electrical discharge

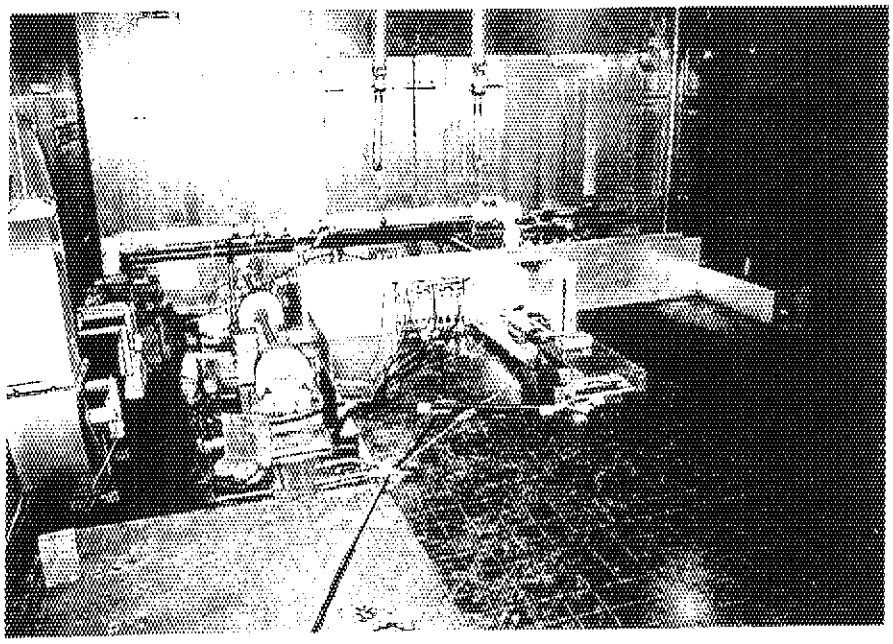

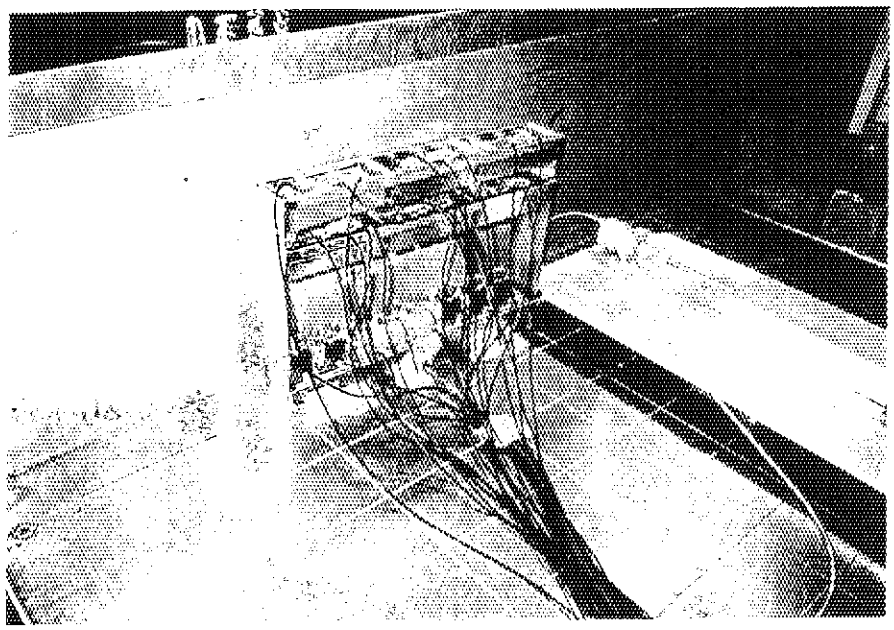

Fig. 3.12 Picture of inspection probe Type-A and Type-B installed on the irradiation table of ^{60}Co irradiation test facility (No.2 Cell in Takasaki Establishment, JAERI)

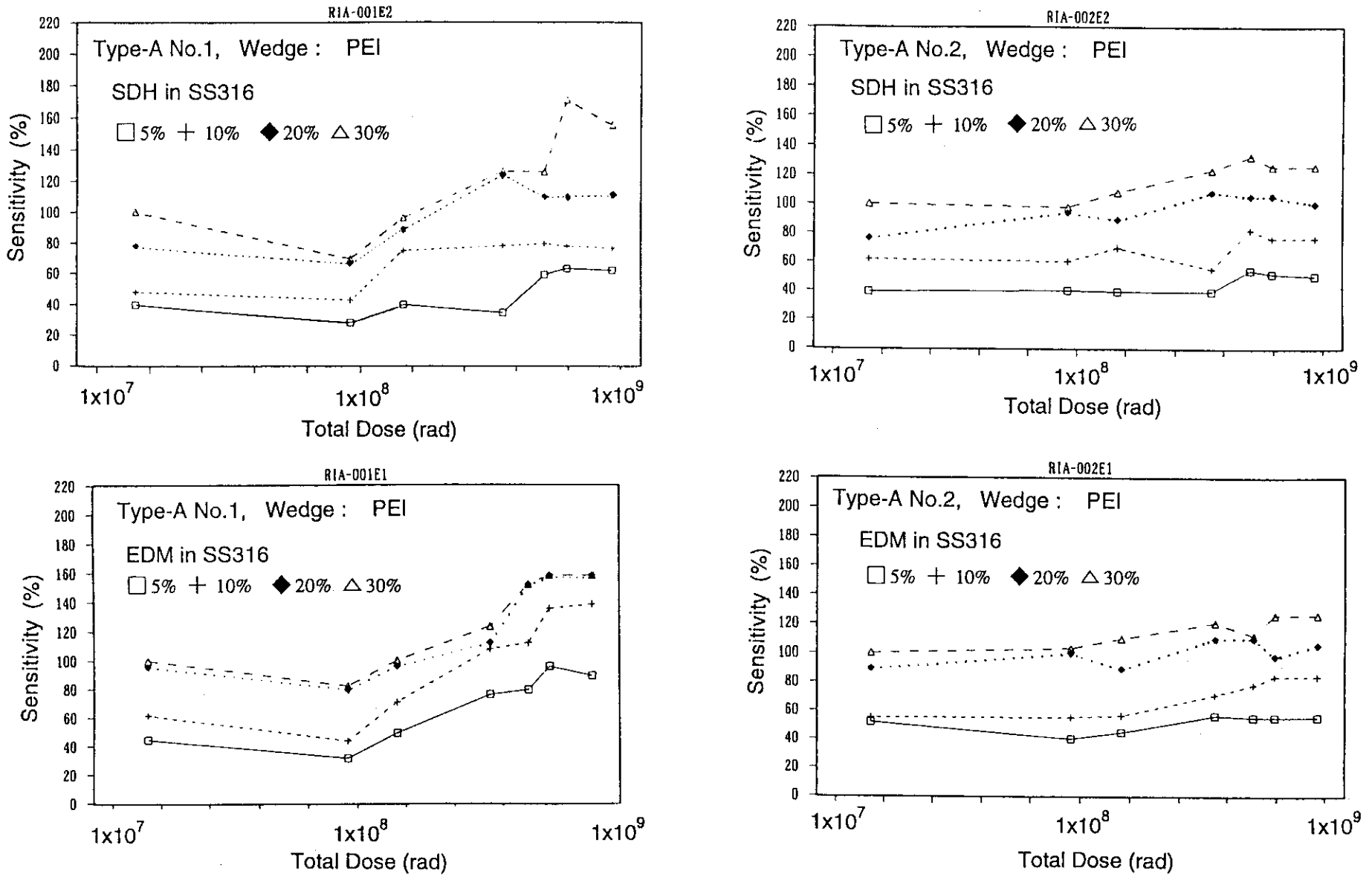

Fig. 3. 13 Change of the sensitivity of inspection probe Type-A due to gamma ray irradiation at 10^6 R/h (1) the change of sensitivity to various size of defects are shown as a function of total dose

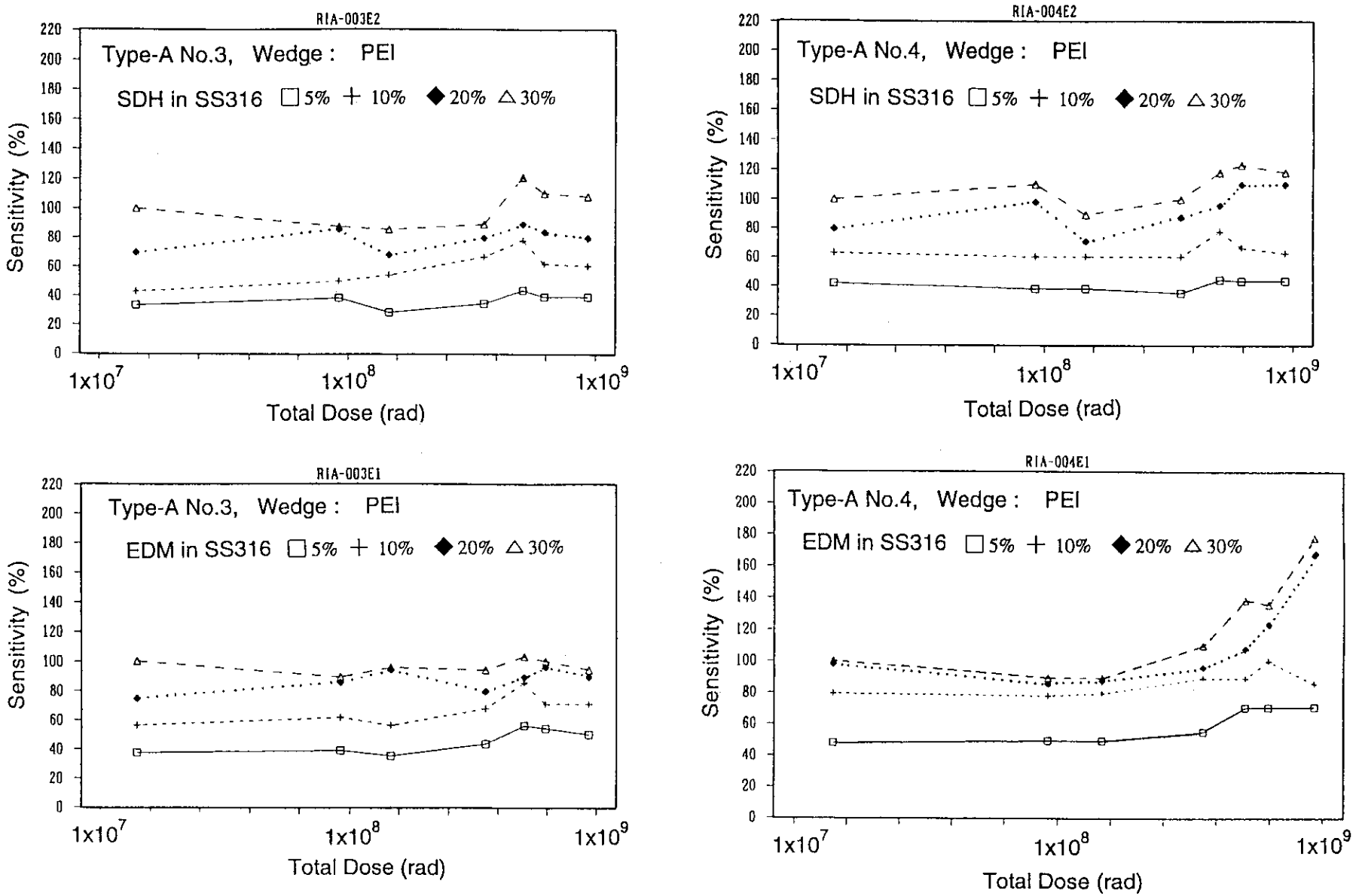

Fig. 3. 14 Change of the sensitivity of inspection probe Type-A due to gamma ray irradiation at 10^6 R/h (2) the change of sensitivity to various size of defects are shown as a function of total dose

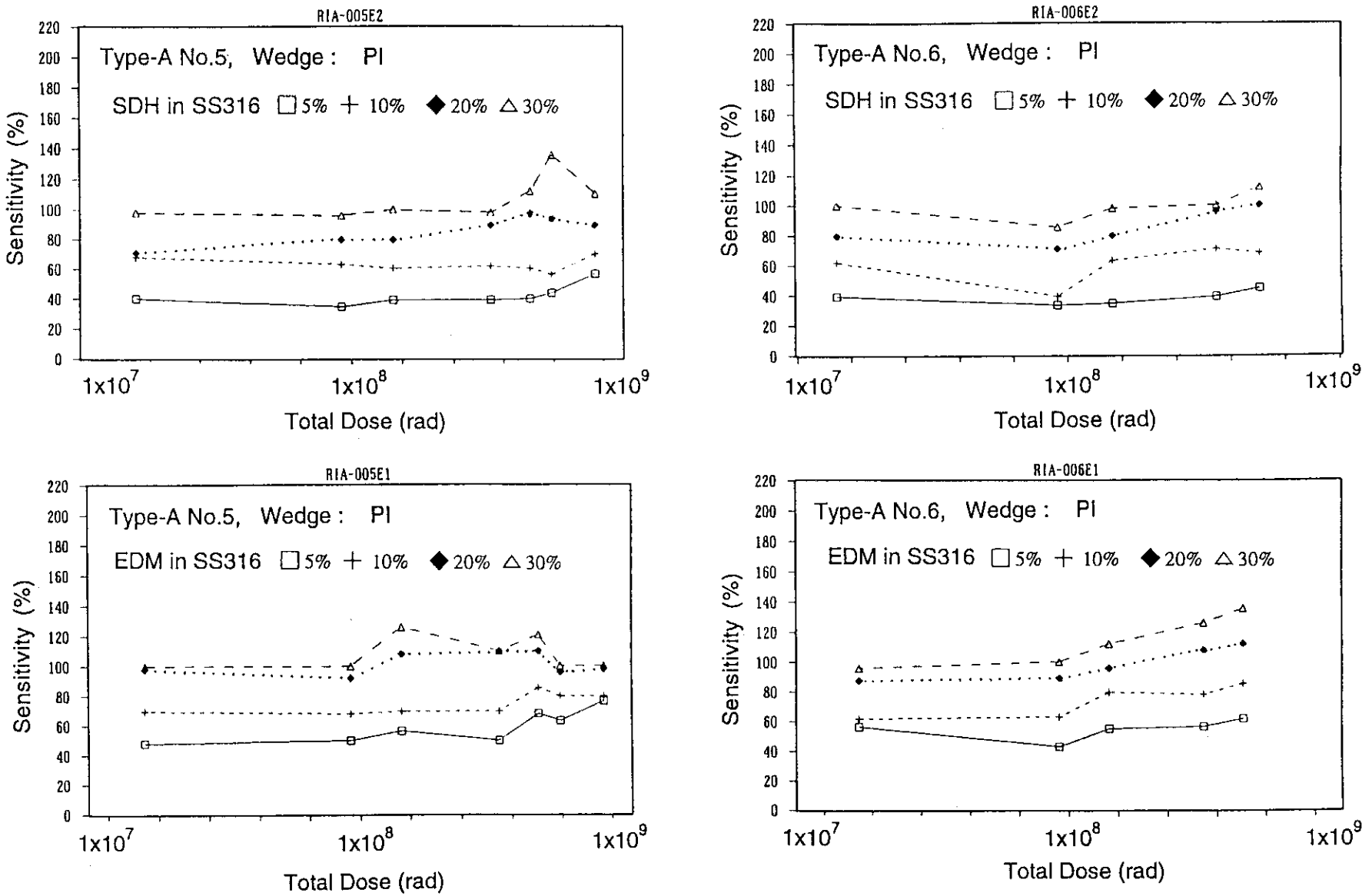

Fig. 3. 15 Change of the sensitivity of inspection probe Type-A due to gamma ray irradiation at 10^6 R/h (3) the change of sensitivity to various size of defects are shown as a function of total dose

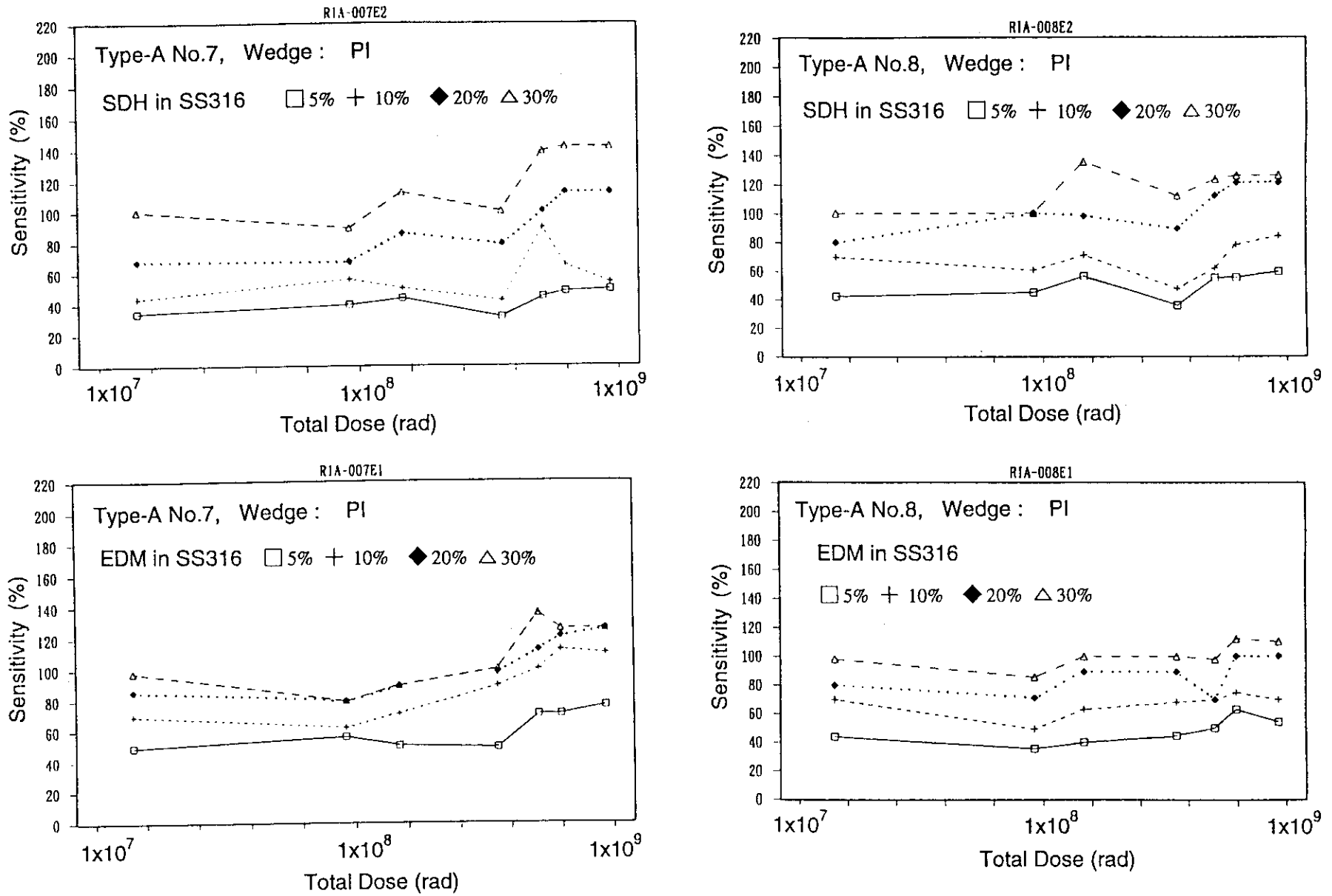

Fig. 3. 16 Change of the sensitivity of inspection probe Type-A due to gamma ray irradiation at 10^6 R/h (4) the change of sensitivity to various size of defects are shown as a function of total dose

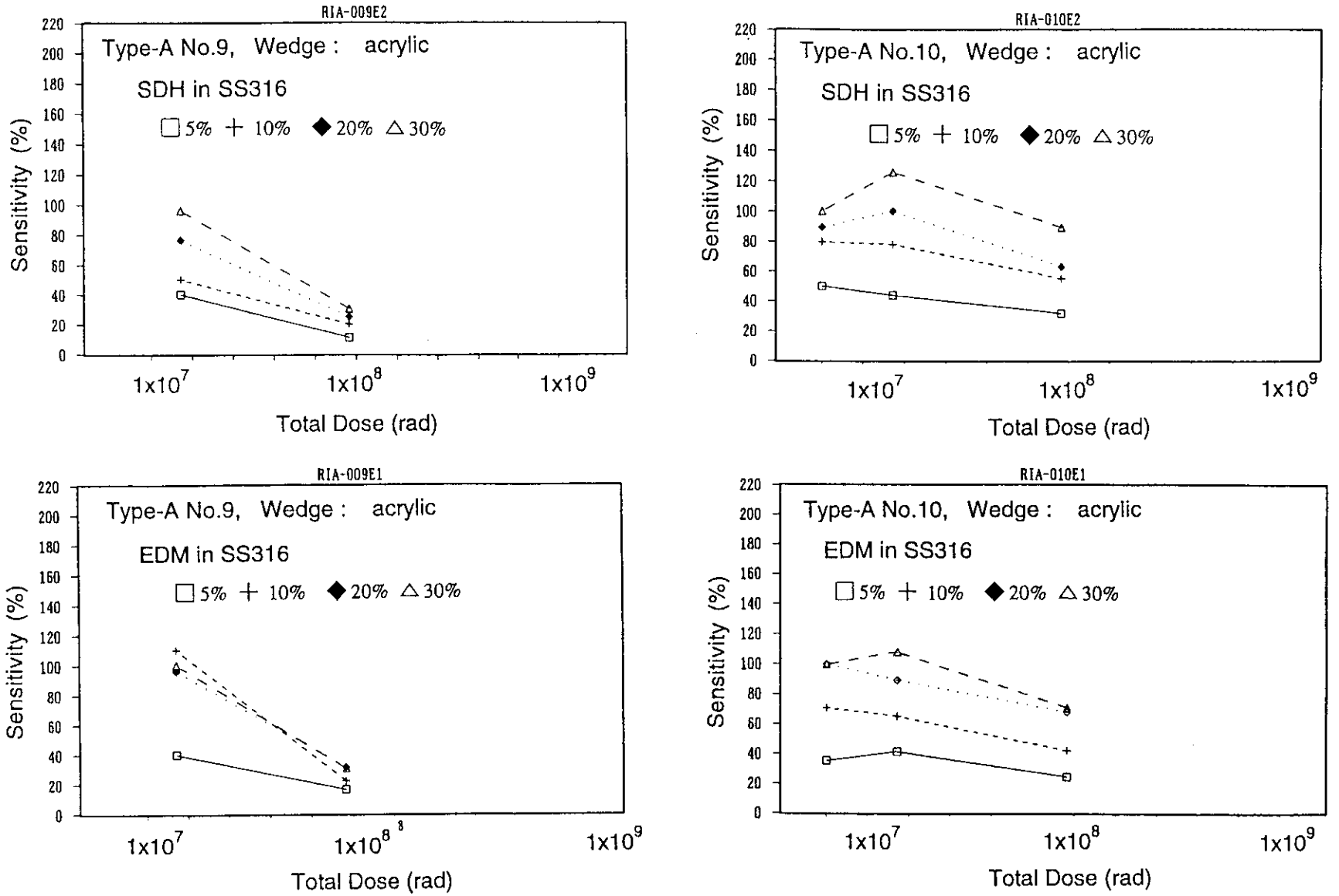

Fig. 3. 17 Change of the sensitivity of inspection probe Type-A due to gamma ray irradiation at 10^6 R/h (5) the change of sensitivity to various size of defects are shown as a function of total dose

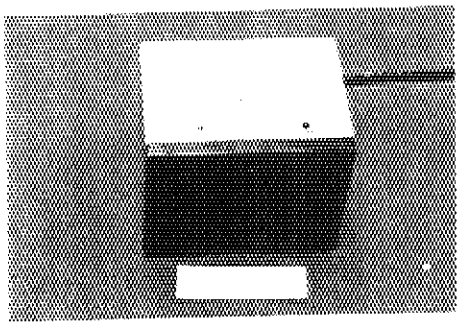

Wedge material : PEI

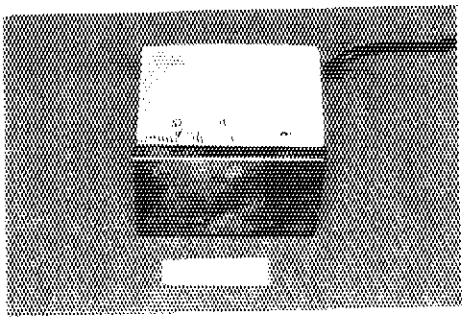

Wedge material : PEI

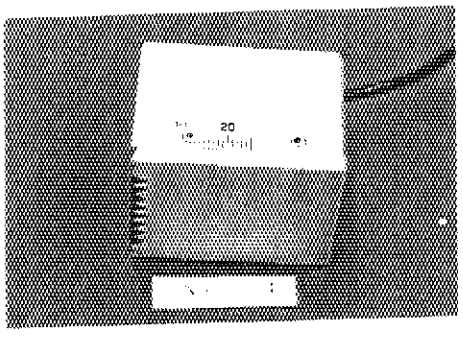

Wedge material : PI

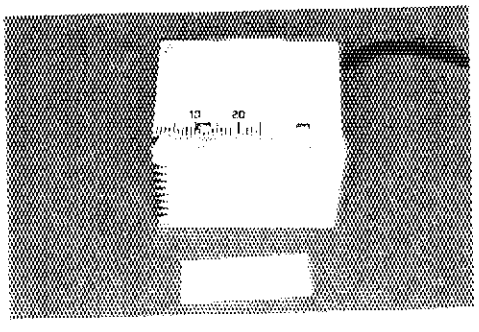

Wedge material : PI

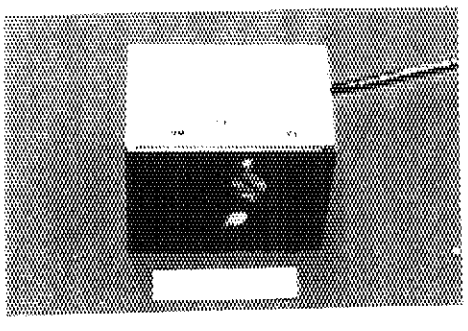

Wedge material : acrylic

a) before the irradiation

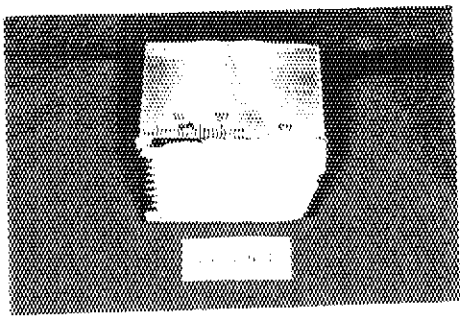

Wedge material : acrylic

b) after the irradiation

Fig. 3. 18 View of angular inspection probe Type-A after the irradiation test up to 1 x 10^9 rad

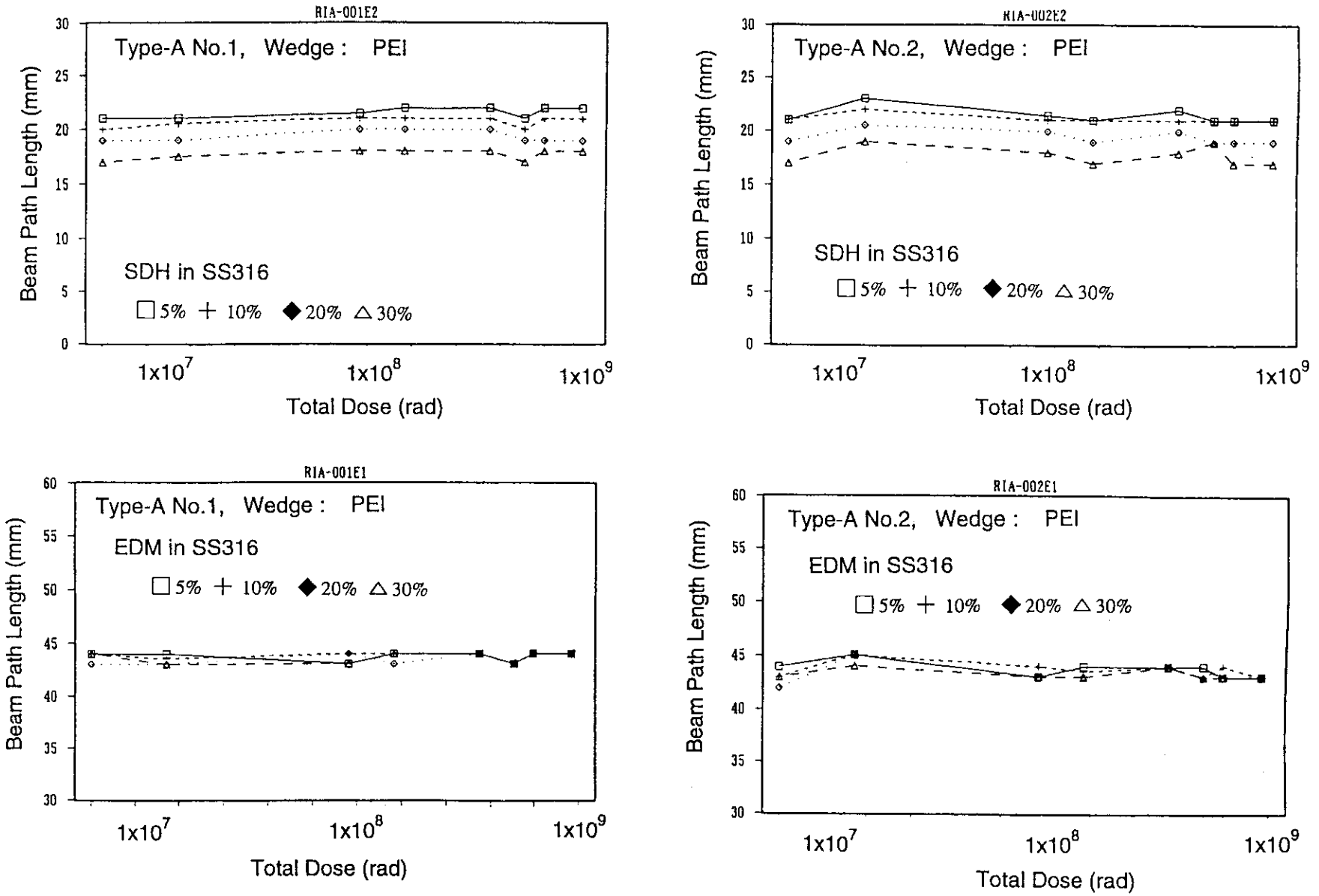

Fig. 3.19 Change of the beam path length of inspection probe Type-A due to gamma ray irradiation at 10^6 R/h (1) the change of beam path length to various size of defects are shown as a function of total dose

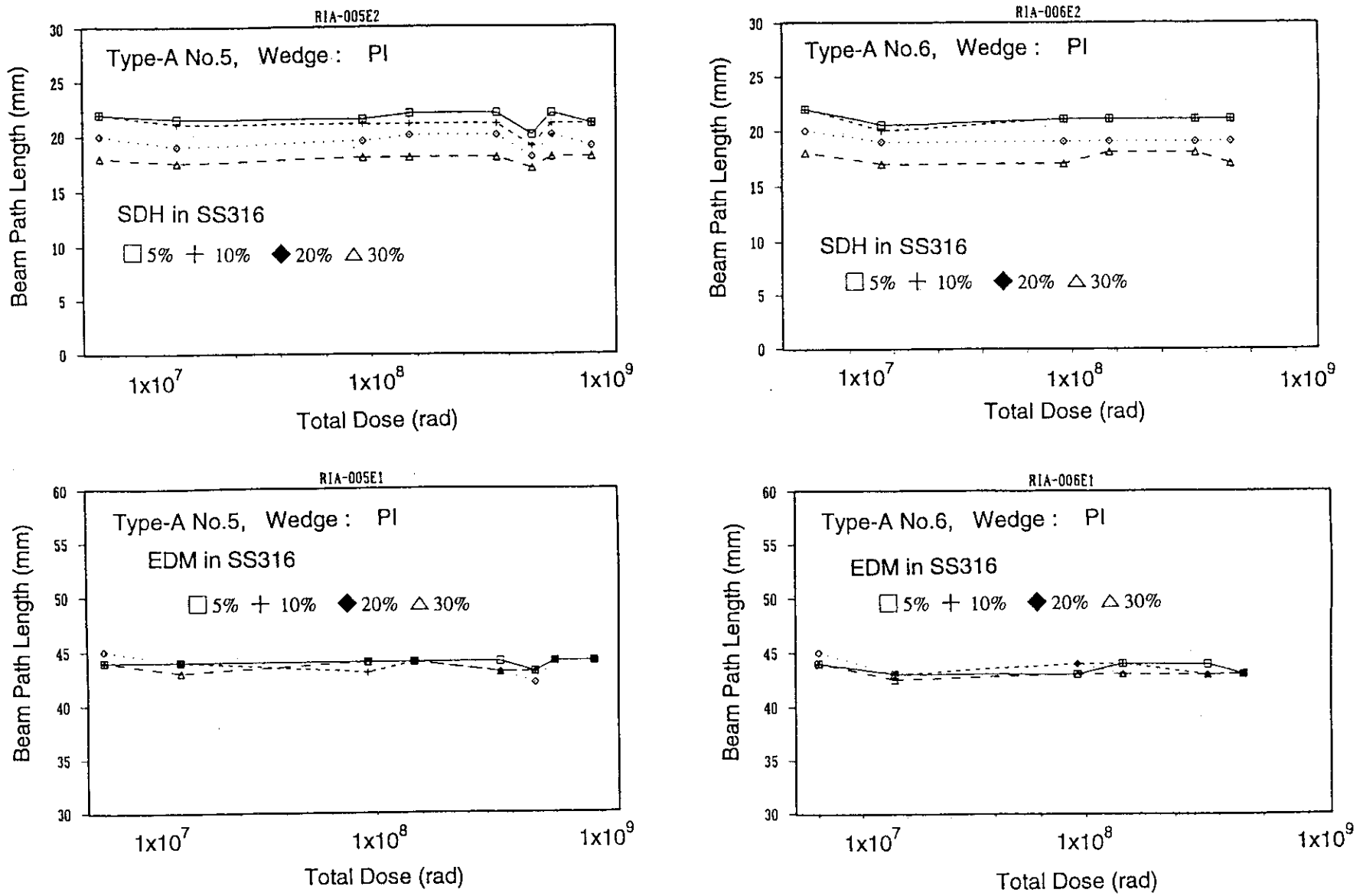

Fig. 3.20 **Change of the beam path length of inspection probe Type-A due to gamma ray irradiation at 10^6 R/h (2) the change of beam path length to various size of defects are shown as a function of total dose**

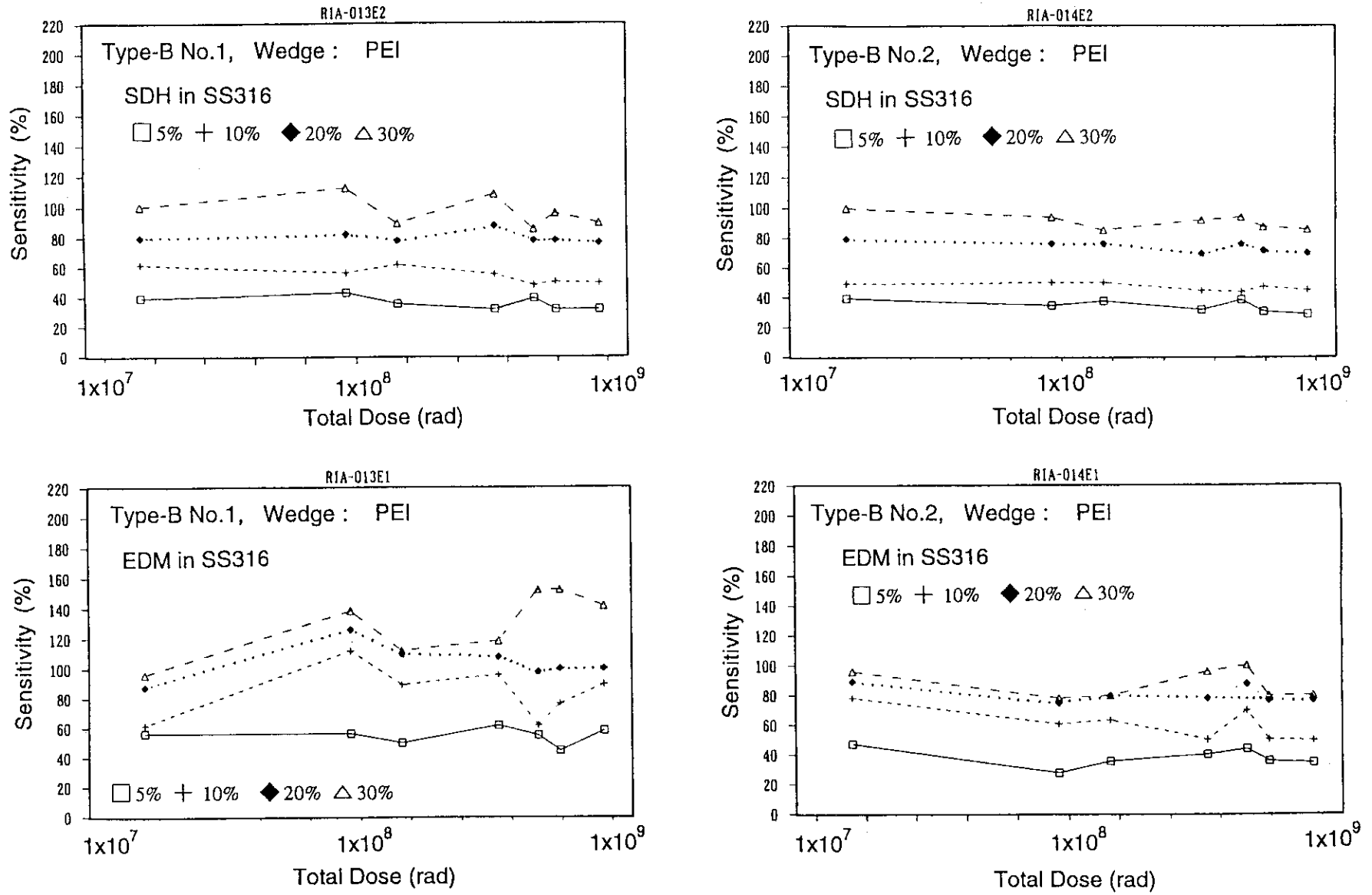

Fig. 3. 21 Change of the sensitivity of inspection probe Type-B due to gamma ray irradiation at 10^6 R/h (1) the change of sensitivity to various size of defects are shown as a function of total dose

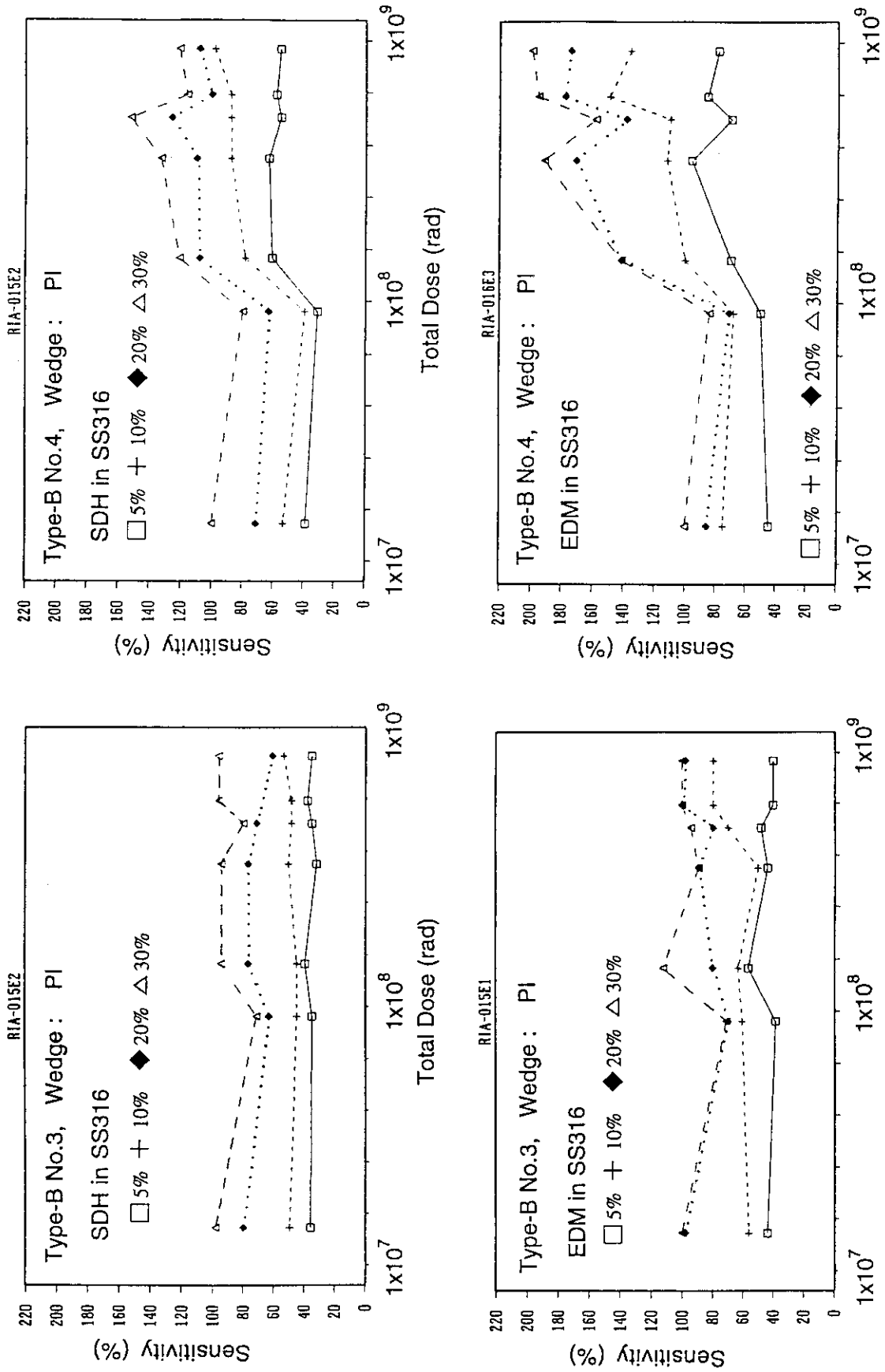

Fig. 3. 22 Change of the sensitivity of inspection probe Type-B due to gamma ray irradiation at 10^6 R/h (2) the change of sensitivity to various size of defects are shown as a function of total dose

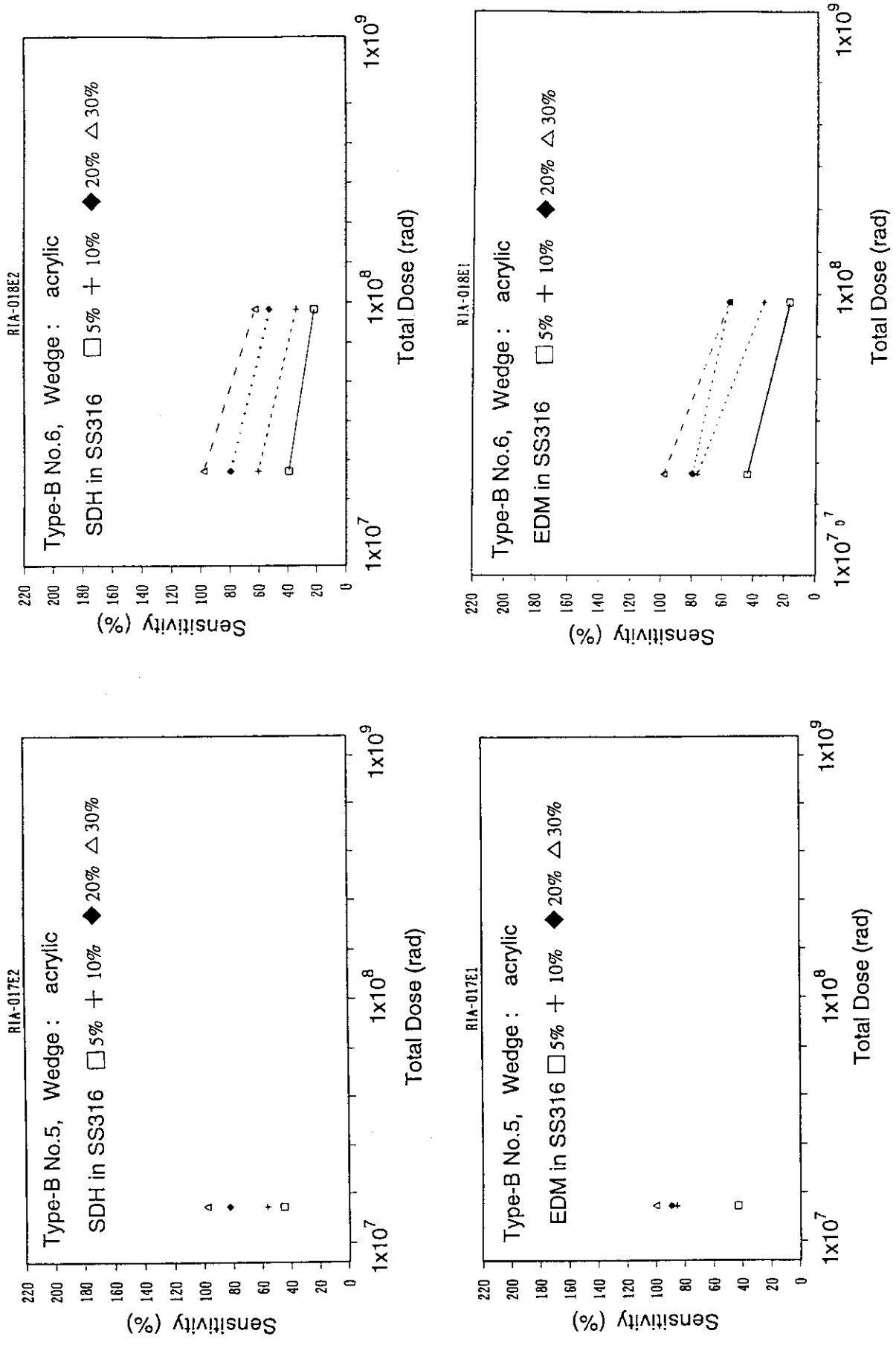

Fig. 3. 23 Change of the sensitivity of inspection probe Type-B due to gamma ray irradiation at 10^6 R/h (3) the change of sensitivity to various size of defects are shown as a function of total dose

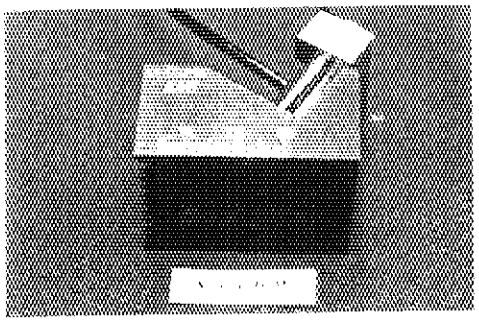

Wedge material : PEI

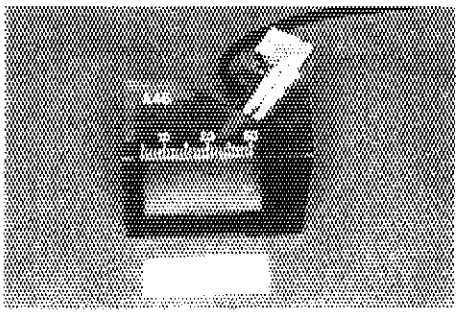

Wedge material : PEI

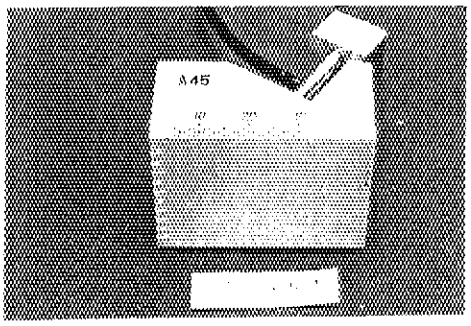

Wedge material : PI

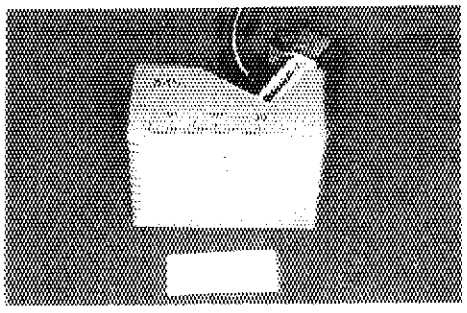

Wedge material : PI

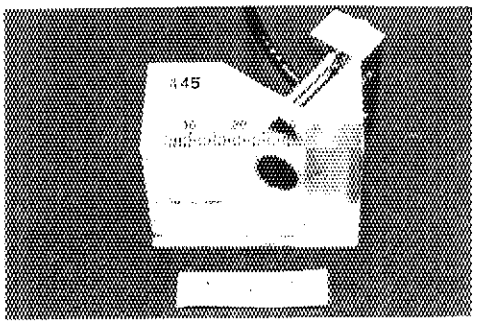

Wedge material : acrylic

a) before the irradiation

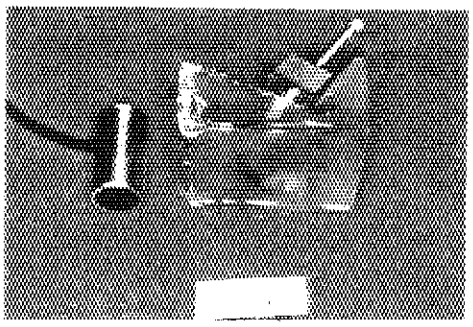

Wedge material : acrylic

b) after the irradiation

Fig. 3. 24 View of angular inspection probe Type-B after the irradiation test up to 1 x 10^9 rad

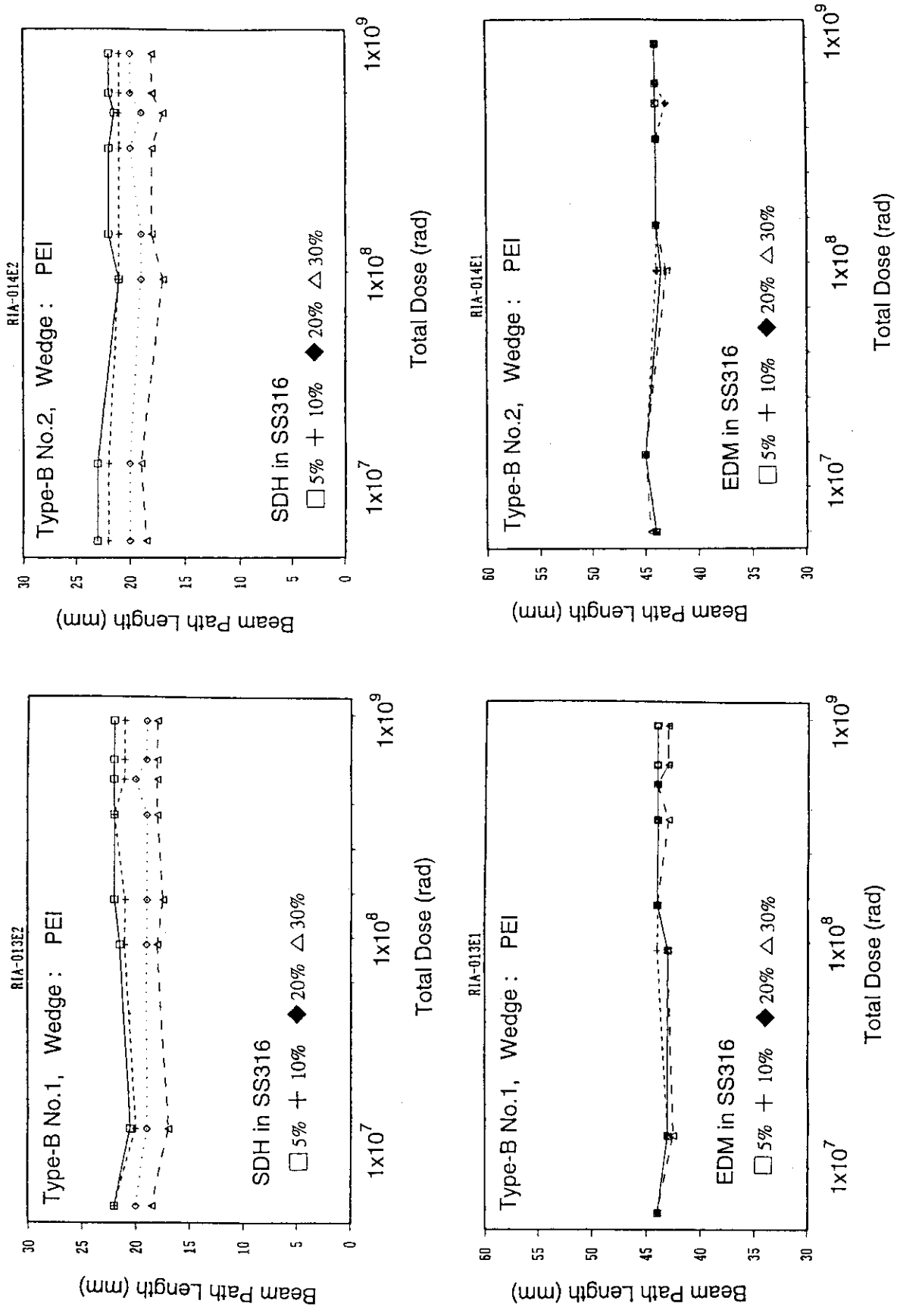

Fig. 3.25 Change of the beam path length of inspection probe Type-B due to gamma ray irradiation at 10^6 R/h (1) the change of beam path length to various size of defects are shown as a function of total dose

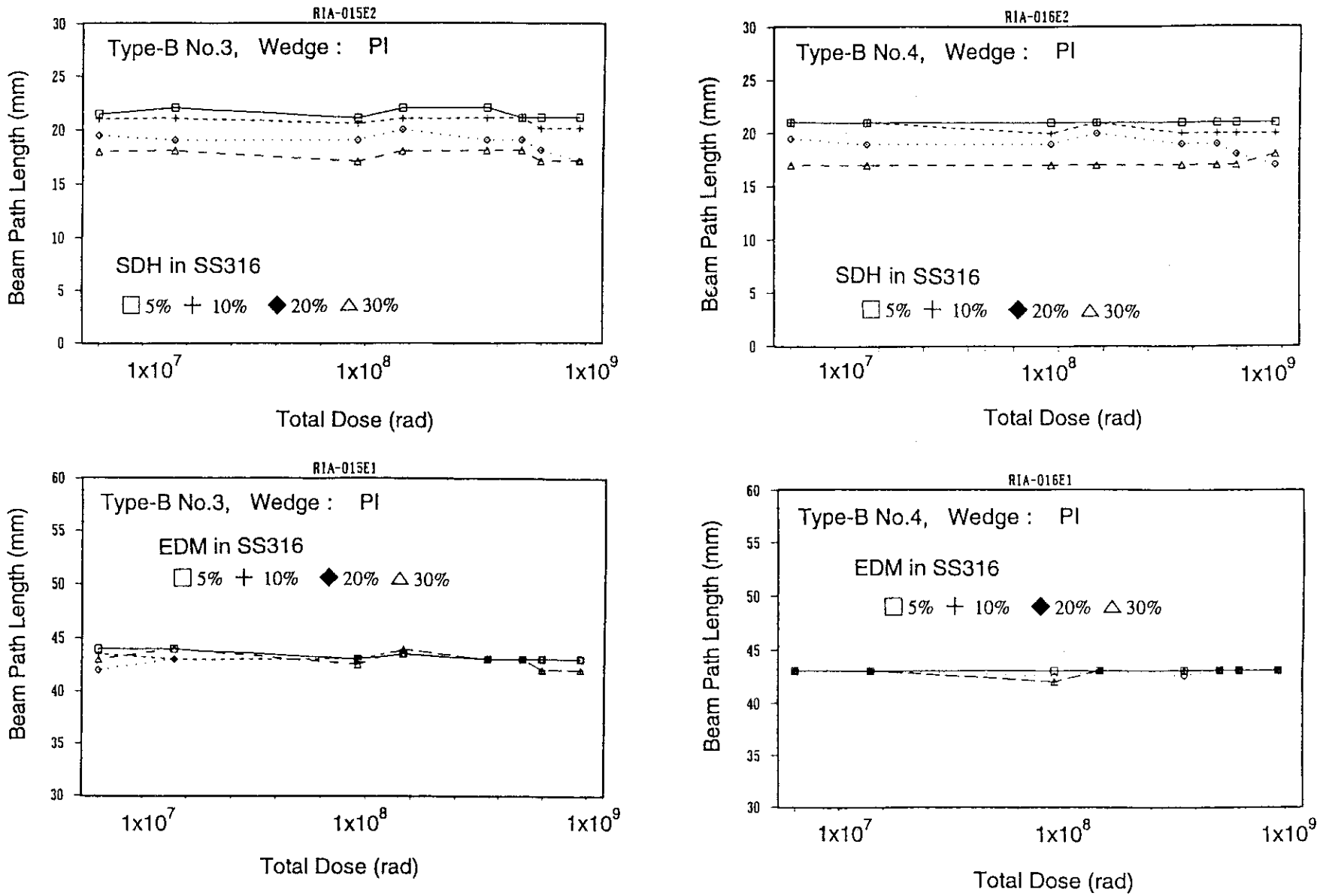

Fig. 3.26 Change of the beam path length of inspection probe Type-B due to gamma ray irradiation at 10^6 R/h (2) the change of beam path length to various size of defects are shown as a function of total dose